SPE/PS-CIM/CHOA 97733
PS2005-327

3D Geomodelling and Flow Simulation of the Late Devonian Bakken Formation in South-Central Saskatchewan - Case Study: Smiley Buffalo Heavy Oil Waterflood

R. Mohr, C.A. Estrada, SPE, and K. Norrena, SPE, Nexen Inc.

This paper was prepared for presentation at the 2005 SPE International Thermal Operations and Heavy Oil Symposium held in Calgary, Alberta, Canada, 1–3 November 2005.

Abstract

A sound geological model, a consistent geocellular model, and flow simulation are all critical components to successful optimization of a heavy oil waterflood project. Despite the availability of a sound geologic model, high quality seismic and abundant core, log, and production data, optimization of the waterflood project at the Smiley Buffalo field in south-central Saskatchewan held many challenges

The primary reservoir at Smiley is the middle Bakken sandstone which was deposited as offshore sand ridges in late Devonian to early Mississippian time. The reservoir structure has been subjected to post-depositional solutioning of the underlying Torquay Formation and karstification which causes reservoir breaks, fracture networks, and irregularities in the saturation functions. These features have important effects on reservoir performance. The geologic model and seismic information were used to construct a consistent structural model. A facies classification model was built with fuzzy logic which used the core and log data as well as the geologic model. Sequential indicator simulation was used to populate the structural model with facies information, and sequential Gaussian simulation was used to populate the petrophysical properties. Representative models were selected for upscaling and flow simulation and subsequent well location selection.

Introduction

A detailed understanding of reservoir behaviour is important for profitable management of mature and declining pools. Geomodelling and flow simulation afford the opportunity to observe reservoir behavior under alternative strategies and help with pool management. The Smiley Buffalo field, located in southern Saskatchewan (Figure 1), is a mature heavy oil reservoir that has complex geologic features that complicate reservoir management. Improved understanding of the Smiley Buffalo field was gained by constructing a geomodel and submitting the model to flow simulation to help to identify areas of missed opportunity. The findings are currently being used for reservoir management decisions.

The predominant complicating feature of the reservoir is that it sits above the carbonate Torquay formation which has experienced post depositional erosion and karstification. The fractures generated during this structural deformation provide conduits for out-of-zone water infiltration and compartmentalization of reservoir regions.

This paper documents the approach used to characterize the reservoir and predict reservoir behavior. The conceptual geological model is covered first, followed by the geostatistical model and then flow simulation.

General Geology

The primary reservoir at the Smiley Buffalo oilfield (Figure 2) is the Middle Bakken sandstone which was deposited as an offshore sand ridge in late Devonian to early Mississippian time. It was one of a series of elongate tidal sand ridges trending NE-SW in west-central Saskatchewan (Figure 1).

The Late Devonian to Early Mississippian Bakken formation in west-central Saskatchewan is a siliciclastic unit which lies above the Devonian Big Valley Formation and below the Mississippian Madison Group carbonates. The thickness of the suprajacent carbonates is extremely variable due to the incision of the pre-Cretaceous unconformity which has removed variable amounts of the carbonates (Figure 3).

The Bakken formation is subdivided into the upper, middle, and lower units throughout Saskatchewan. The lower and upper Bakken are composed of finely-laminated, highly organic rich black shale. They tend to be homogeneous, waxy, fissile to well indurated, non-calcareous to slightly calcareous, pyritiferous, and uraniferous.[1] The shales provided good marker beds as they are consistently present throughout the study area.

The middle Bakken sandstone, which forms the reservoir facies, is a fine to very fine-grained, friable, unconsolidated to semi-unconsolidated quartz sandstone. The sandstone is capped by the impermeable upper Bakken shale.

Deposition began when marine currents carved a ridge and

swale morphology (Figure 4) on the shelf with scattered bathymetric irregularities on the surface. Bathymetric highs lying oblique to current flow provided a nucleation site for all available sediment and ridge formation began.[2] The Huthnance process is a widely accepted theory used to explain both ridge formation and migration over time.[2,3,4] In simplest terms, the Huthnance process begins when an irregularity or bathymetric high forms on the shelf surface. Currents flowing oblique to these irregularities erode the up-current side and deposits sand on the down-current side (Figure 5) causing upward growth and/or down-current.[2] Snedden and Dalrymple (1999) proposed the following four conditions that are necessary for ridge formation: (1) a sufficient supply of loose sand much be present; (2) currents capable of moving the sand; (3) a pre-existing irregularity must exist to act as a nucleus for ridge formation; and (4) sand must remain exposed on the sea floor long enough to be molded into ridge complexes. As long as these criteria are met, formation of these shelf sand ridges can take place.

The rate at which these ridges accumulate and migrate is thought to be a directly related to variations in magnitude, frequency, and orientation of the waves and currents.[5] However, the quality of the sand building these ridges depends greatly on the sediment being supplied to the shelf during their deposition. For instance, if sand supply is restricted, the ridges are still able to accrete vertically but their width will substantially decrease. This results in a decreased areal extent of good ridge sands (reservoir) and an increased areal extent of the tighter, siltier, inter-ridge facies.[2] Therefore, sand supply was perhaps the most important control on reservoir distribution and quality at Smiley Buffalo.

Overall, conditions similar to this existed during the late Devonian to Early Mississippian time throughout in west-central Saskatchewan and allowed the middle Bakken sandstones to be deposited. Variations in sediment supply led to a variation in sand quality throughout the Smiley Field leaving a very geologically complex reservoir to waterflood. Therefore, 3D geomodelling was a logical step to try and understand the observed heterogeneity.

Facies Definition

The prerequisite to completing any modelling work requires that all available core be interpreted and a clear and defined set of facies which accurately delineate the reservoir complexity be proposed. Seven facies types were defined using all available core in the study area (Figure 2). They consisted of the following:

1. Bioturbated Sandstone (Figure 6)

- Variable reservoir quality. Generally low porosity and permeability.

2. Ridge Sandstone (Figure 6)

- This primary reservoir facies has good to excellent reservoir quality with 25-35% porosity and Darcy permeabilities.

3. Inter-Ridge Sandstone with 0.5-1 cm. thick inter-bedded silts (Figure 6)

- Variable reservoir quality. 17-23% porosity and 2-2300 md permeability.

4. Inter-Ridge Sandstone with 2-5 cm. thick inter-bedded silts (Figure 6)

- Variable reservoir quality, generally poor. The better samples have up to 36% porosity and 2- 2000 md permeability.

5. Precursor sandstone (Figure 6)

- Poor reservoir quality. Lies at the base of the Middle Bakken Section.

6. Calcite cemented sandstone (Figure 6)

- Poor to nil reservoir quality. Discontinuous throughout the study area

7. Green Siltstone Facies (Figure 6)

- Non flow unit capping the Middle Bakken sandstone sequence.

At the base, the calcite-cemented sand/coquina is seen in numerous core varying from fine grained calcite cemented sand to a bioclastic coquina facies. This unit typically ranges from 1-2 meters thick when present.

The precursor facies is a fine to very fine-grained quartz sandstone with high concentrations of inter-bedded silts. Unidirectional ripple lamination and light oil stain is seen throughout. The precursor facies both in core and petrophysical logs looks extremely similar to the inter-ridge facies which lie above it. Therefore, in order for it to be defined as a pre-cursor facies, it must lie immediately above either the Lower Bakken Shale or the calcite cemented zone. If ridge sands lie subjacent to it, then the assumption was made that the ridge had migrated enough to eliminate the pre-cursor facies completely. As a result, this unit is defined both on stratigraphy as well as lithology.

The inter-ridge sands at Smiley are fine to very fined-grained sandstone inter-bedded with silts clearly demonstrating a unidirectional ripple lamination. Thicknesses vary from 1-5 meters but can appear much thicker on petrophysical logs. On examination of core, it was observed that silt beds vary in thickness but on a relatively consistent basis. Consequently, the interval was broken up into inter-ridge facies with silt inter-beds which varied from 0.5-1cm thick and inter-ridge facies with silt inter-beds from 2-5cm thick (Figure 6). Later in the modelling stage, it was realized that petrophysically this difference in silt thickness was difficult to consistently differentiate. Because we considered both of these units to be "non-flow" units this did not pose a problem for all the rest of the modelling process.

The Ridge Sand (reservoir) facies is a higher energy fine-grained, moderate to well sorted, semi to unconsolidated quartz sandstone. Unidirectional ripple lamination can be

distinguished in gas zones where oil stain doesn't conceal the sedimentary structures. The ridge sandstone facies is considered to be the dominant flow or reservoir unit and therefore is an extremely important facies both to understand and predict.

The bioturbated zone lies in the upper most section of the Middle Bakken and varies in thickness relative to geographic location in the ridge and swale environment (Figure 4). The bioturbated thickness increases closer to the swale features and is relatively thin on the axes of the ridge. Bioturbated ridge sands are significantly lower in porosity (<21%) and were therefore considered a non-flow unit.

Above the bioturbated sands is a slightly bioclastic green siltstone. This unit tends to be quite thin and is reasonably continuous across the field. For modelling purposes, this facies was also considered to be a non-flow unit.

All of the above facies types were built into the geological model but only the Ridge Sandstone (reservoir) Facies was considered a flow unit and is therefore the main control on the flow simulation.

Reservoir Structure

The middle Bakken formation has been subjected to extensive post-depositional karstification due to dissolution and collapse in the dolomitic limestones of the Torquay formation (Figure 8). From seismic interpretation, it is interpreted that the majority of solutioning took place after deposition of the middle Bakken and prior to deposition of the Mannville formation. There tends to be no sign of drop above the Mannville horizon on the majority of the seismic data and thus it is inferred that the majority of this movement happened prior to the Mannville deposition.[6]

The sinkholes associated with karstification leads to significant complications in managing and modelling the field through compartmentalizing the reservoir and allowing the intrusion of out-of-zone water. The resulting fractures have caused early breakthrough of injection water in producing wells and is also potentially providing a direct path to a thief zone for injected water.

Two approaches were considered for handling the sinkholes. The first was to attempt to reproduce the sinkholes using a system of faults and the second was to treat the sinkholes as a system of topographic lows. It was concluded that modelling the sinkholes as faults would be difficult and that the topographic lows approach would afford better opportunities to account for out-of-zone water.

Seismic information was used to build the horizon for the top of the middle Bakken.[6] The other horizons (the green siltstone, reservoir facies, precursor and calcite cemented horizons) were constructed from isopach maps that were built using a combination of seismic information and the corresponding well markers.

The first attempt to build the structural model used a minimum curvature algorithm[7] for the horizons and isopach maps. The resulting grid had twisted cells and cells with negative volumes. Even with several variations of the parameters, the grid did not improve. The data was exported and the surfaces built using the GSLIB kriging program (KT3D).[8] The kriged surfaces generated a grid without anomalies and the final structural model was verified by comparing it to seismic cross-sections. A subset of the grid was extracted for lithological and petrophysical modelling that contained only the reservoir zone.

The final structural model consisted of 2 horizons, the bottom of the green siltstone and the top of the precursor or calcite cemented horizons (where pre-cursor had been completely eroded), and a single zone. The grid is a fine scale grid with cells that measured 20m x 20m x 1m with 2.88 million cells.

Petrophysical Model

There are 134 wells in the data set (Figure 2). Eighteen of the wells have core with a complete core analysis including total porosity, air permeability, grain density, and residual oil and water saturations (Figure 2). None of the wells showed a definitive oil/water contact, and 19 of the 134 wells show a gas/oil contact in either the Mannville or Bakken formations. Log analysis was completed keeping this in mind and calculations for gas, oil, and water saturations were completed.[9]

Once the log data had been collected and cleaned, the first step was to develop a relationship between the lithology logs and petrophysical logs (gamma ray, neutron, density logs, and photo electric logs) using a combination of statistical and deterministic program methods. The derived relationship was then applied to generate a set of electrofacies, or log derived facies, for every un-cored well in the study area (Figure 7). Multiple iterations were undertaken by predicting facies in known (i.e. cored) wells and comparing that prediction to the actual lithology interpretation. When an acceptable match was acquired between actual and predicted, the process was applied to all wells. This process essentially created a synthetic core for every un-cored well.

Obtaining a facies track for modelling was an iterative procedure. The first attempt gave facies that violated the distribution of petrophysical properties defined in the conceptual geologic model. The core based facies classifications were revisited and a new model generated. The new model was better, but it still had to be hand edited to remove anomalies. The facies information was upscaled to the grid using the most probable classification criteria. The input and block averaged proportions are shown in Figure 9. About 40% of the zone is Facies 2, 23% Facies 3, 22% Facies 4, and 15% Facies 5.

Biased core sampling in the inter-ridge facies (Facies 3&4) was a concern. Facies 3 and 4 both have alternating beds of fine grained quartz sandstone and silt beds. Samples were

extracted mostly from the sandy intervals in these facies and silts were ignored. The consequence was biased distributions of permeability and porosity in the inter-ridge facies. The bias was treated in the calibration of the logs petrophysical attributes to the core data.

Log derived permeabilities were calculated using a relationship derived from multiple regression of core Kmax values against wet clay volumes. A satisfactory match was derived between core and log permeabilities. Porosity and fluid saturations were determined using probabilistic log analysis. The input logs included neutron, density, deep resistivity, gamma ray, and photo electric logs in the newer wells.

Water saturations were calculated using key parameters of: Rw=0.36 ohm-m at 25 degrees C, Cwb=1ohm-m at 25 degrees C, a=1, m=1.8, and n=1.8. The water resistivity was obtained from drill stem test analysis. An "m" value of 1.8 was obtained by matching the core and log oil saturations in clean sand. The key observation made was that there is no true wet zone observed at Smiley Buffalo which made it very difficult to do any complex fine tuning of water saturation models. Median log-derived water saturations are: 36% for Facies 2, 46% for Facies 3, and 72% for Facies 4. [9]

The upscaling of petrophysical attributes to the grid was arithmetic for porosity and water saturation. Geometric upscaling was used for permeability because it did the best job of reproducing the shape of the distribution. The upscaling was biased on facies, i.e., a block upscaled to Facies 2 used only values derived from Facies 2 information on the log.

The raw and upscaled porosities for all facies is shown in Figure 10. The average raw porosity over the field and all facies is 22.5% and the upscaled is 23.84%.

The raw and upscaled distributions for permeability are shown in Figure 11. The raw permeability is 884mD, and the upscaled 827mD. We acknowledge that there are more robust techniques for upscaling permeability, pressure solvers for example, but there was not sufficient time to explore these options.

The raw and upscaled distributions of water saturation are shown in Figure 12. The average raw water saturation is 47% and the upscaled is 48%.

The modelling approach was kept simple. Sequential indicator simulation was used to construct the facies realizations, sequential Gaussian simulation was used to construct the porosity realizations, and colocated cosimulation was used to construct the immovable water and permeability realizations. The sinkholes made it difficult to discern any areal trends on any of the attributes so none were used. A vertical proportion trend was used for facies modeling. There is poor correlation between porosity and depth (ρ=0.35), and depth and permeability (ρ=0.25), nor were there any obvious trends.

Facies 3 and 4 had similar distributions of petrophysical attributes and variograms and are both nearly non-reservoir so they were lumped together for modeling and called Facies 4. The petrophysical properties were normal scores transformed for the purpose of semivariogram modeling. The sequential Gaussian simulation algorithm performed the normal scores transforms internally.

The Tables below tabulate the semivariograms used for facies, porosity, permeability, and water saturation, respectively. The "Type" column refers to the semivariograms numerical model, "Sph." is a spherical semivariogram model, and "Exp." is an exponential model. The semivariogram ranges are given in meters. "Maj." is the direction of major continuity, "Min." is the direction of minor continuity, and "Vert." is the perpendicular to the major and minor directions.

Table 1 - Facies semivariograms

Facies	Type	Nugget	Maj. Dir.	Maj. Range	Min. Range	Vert. Range
2	Sph.	0.047	N41E	535	375	5
3	Sph.	0.046	N21W	750	390	2
4	Sph.	0.13	N135E	370	270	5

Table 2 - Porosity semivariograms

Facies	Type	Nugget	Maj. Dir.	Maj. Range	Min. Range	Vert. Range
2	Exp.	0.01	N47E	1365	615	8
3	Exp.	0.01	N60E	1065	610	10
4	Exp.	0.01	N140E	690	500	7

Table 3 - Permeability semivariograms

Facies	Type	Nugget	Maj. Dir.	Maj. Range	Min. Range	Vert. Range
2	Exp.	0.01	N35E	700	580	9
3	Exp.	0.01	N35E	640	425	8
4	Exp.	0.01	N120E	580	230	7

Table 4 - Water saturation semivariograms

Facies	Type	Nugget	Maj. Dir.	Maj. Range	Min. Range	Vert. Range
2	Exp.	0.01	N40E	430	310	10
3	Exp.	0.01	N10E	640	475	9
4	Exp.	0.01	N50E	260	200	5

Note that there is little nugget effect in the semivariograms. The selection of such small nugget effects may understate reservoir heterogeneity. Except for water saturation, the semivariogram parameters echo the geologic conceptual model; the direction of maximal continuity is along the long axis of the reservoir.

The global relationship between porosity and permeability is nearly functional (Figure 13). There is fairly good separation between each of the facies types. Facies 4 has consistently

low permeability's and porosity. Facies 2 and 3 overlap, with most of the Facies 2 points falling in high permeability regions. The permeability-porosity relationship is nearly functional. We could have used a functional relationship to model permeability's but opted to use colocated cosimulation with porosity as the secondary variable to add in heterogeneity that was lost in the calibration of log data. For Facies 2, 3, and 4, the following correlation coefficients were used: P=0.94, 0.97, and 0.95, respectively. A variance reduction of 90% percent was applied because this value reproduced the permeability histograms best.

Water saturation was highly variable (Figure 14). Figure 15 shows a scatterplot of Facies 2 and 3. The correlation coefficient for this scatterplot is about ρ=-0.3. This correlation coefficient was used to model water saturation for both Facies 2 and 3. Water saturation for Facies 4 was modelled as a constant 100%.

A reservoir boundary was determined by using a threshold on the kriging variance for a map of arbitrary values located at the well locations. Uncertainty in the reservoir extent was not considered in the model of uncertainty. The reservoir model was clipped according to this boundary.

Approximately 100 realizations of each attribute were generated. The realizations of the reservoir model of uncertainty were ranked according to stock tank barrels in place. The attribute distributions for the 10^{th}, 50^{th}, and 90^{th} realizations were compared to ensure that the mean, variance, and shape were reasonable.

The 50^{th} realization was selected for flow simulation studies. An areal map of this is shown for facies (Figure 16), porosity (Figure 17), permeability (Figure 18) and water saturation (Figure 19) realizations. The realizations were exported for submission to flow simulation.

Flow Simulation

The 2.8 million cell fine grid geometry was upscaled by increasing the areal dimensions by a factor of 2. The vertical resolution of the grid, a total of 18 layers with average thickness of 1.1 m, was kept. The upscaled grid has dimensions of Nx*Ny*Nz = 180x141x18 with average grid block size of Dx*Dy*Dz = 50m x 50m x 1.1m. There are 90493 active cells.

Geometric and arithmetic permeability upscaling procedures were applied. Arithmetic permeability upscaling was chosen because it gave well flow capacities more representative of the flow capacity determined from well testing.

Figure 20 shows an example of the permeability profile obtained by different upscaling procedures as compared to the fine grid model. The information corresponds to cored well 01/08-15-32-25W3M. Geometric and harmonic upscaling procedures underestimate the well flow capacity. For the example well, the fine model flow capacity of the perforated interval was 14520 mD-m, whereas the flow capacities of the geometrical and arithmetical permeability upscaled models at the same location were 14376 and 7810 mD-m, respectively.

After applying the arithmetical upscaling, the average permeability of the reservoir, weighted by pore volume at initial conditions, was 1.3 D. If only the main reservoir facies, Facies 2, is considered, then the average permeability is 1.8 D. Average porosities for the whole model and for Facies 2 were only 0.238 and 0.263, respectively.

Vertical permeability was not modelled in the geostatistical study. Using core information from the Cactus Lake Bakken heavy oil field (Figure 1), it was determined that for the main reservoir facies, the average ratio of vertical to horizontal permeability, Kratio, is 0.6. The vertical permeability, Kv, of cells with Facies 2 was made equal to 0.6*Kh in the simulation model. For grid block cells with Facies 3 to 5, Kratio can be considerably smaller than 0.6 due to shale interbedding. Therefore, for cells with Facies 2 to 5, which were grouped as rock type 2, Kratio was used as a history matching parameter.

A rock compressibility of 4.5 x 10^{-6} kPa^{-1} was determined in the laboratory for Bakken samples of the Court (Figure 1) heavy oil Bakken reservoir.

Initial Conditions

Initial reservoir pressure and temperature were Pi = 7205.8 kPaa at -87 m tvdss and Ti = 27.2°, as determined from a DST test performed in section 35-32-25W3M in October 1977. Additional selective Bakken DST data prior to the start of production at Smiley Buffalo was not available. However, DST data from 31/6-17-32-24W3M, a well approximately one section away from the Smiley-Buffalo field, gave a reservoir pressure of 7097.6 kpaa at -87 m. Although the difference between the two measurements is greater than the error attributable to the resolution of the gauge (approximately 50 kpa), the values are close enough to support the use of a single value (7205 kPaa) for initial reservoir pressure for the entire Smiley-Buffalo field. By September 1997, 20 years after the start of production, 280000 m^3 of oil, 872000 m3 of water had been produced, and 1100000 m^3 of water had been injected. Between September and December 1997, DST's recorded in Sections 31-32-24W3M and 32-32-24W3M, where no well had been drilled before, gave static pressures between 6500 and 7000 kPaa which also support our use of 7205 kPaa as the initial reservoir pressure. Fluid properties were measured in a recombined sample collected in May 1978. Recombination was done such that the sample was at its saturation pressure at initial reservoir conditions.

PVT data indicated that oil and gas gravities were 13.2 °API and 0.59, respectively. Other reservoir fluid characteristics are: initial solution gas-oil ratio 20.03 sm^3/sm^3, initial oil volume formation factor 1.041 rm^3/sm^3; and oil viscosity at initial conditions of 743 mPa.s. Figure 21 shows the oil PVT properties as a function of pressure at reservoir temperature.

Fluid Contacts

An initial gas-oil contact at -87 m tvdss was determined from

well logs at structurally high wells drilled between 1977 and 1979 in Sections 29-32-24W3M, 30-32-24W3M and 35-32-25W3M. A different gas-oil contact, -89.5 m tvdss, was detected in Section 05-24-32-25W3M in May 1983. This was not necessarily an original fluid contact because neighboring well 08-23-32-25W3M had started production in 1981. Because the top of Bakken formation in other sections of the field is lower than -87 m and no lower initial gas-oil contacts where identified, with exception of the -89.5 m mentioned above, there is sufficient support for a single initial gas-oil contact value equal to -87 m for the whole Smiley Buffalo field.

Following an initial period of depletion, water injection started in June 1988 in 21/11-29-32-24W3M, then in 21/08-30-32-24 in January 1991. Other areas of the field were developed by primary production until 1998 when additional water injection was implemented. Expansion of the gas cap occurred during that 20 year period, and gas-oil contacts between -92 and -103 m tvdss, were monitored at different locations in the drilling program of 1997-1998.

Although water zones could not be detected in the petrophysical study, water production occurred in several wells before the start of water injection. For example, Figure 22 shows the production history of well 01/08-15-32-25W3M which was the first injector in its section. The LKO from logs and tests is -106.6 m tvdss at 07-23-32-25W3M and 08-15-32-25W3M. A water zone was identified in 41/03-31-32-24W3M below -116.5 m tvdss. The position of the water-oil contact, between -106.6 and -116.5 m, was used as a history matching parameter. The water zones are located in the structurally low areas caused by sinkhole dissolution and collapse of underlying formations.

For clarity, simulation results of Sections 15 to 24 only, will be presented. The grid corresponding to that sector is shown in Figure 23.

The position of the initial gas-oil and water-oil contacts are presented in Figure 24. Water-oil contacts are based on the history matching results. Inactive cells in the interior of the grid are due to very deep sinkholes which are considered to act as barriers to flow.

Special Core Analysis

Two-phase, oil-gas and oil-water, unsteady state relative permeability curves had been measured with Bakken reservoir fluid and rock samples in 1980. Unfortunately, those samples were damaged during the test procedures as evidenced from the very low value of Ko(Swi) and changes in Ko(Swi) from one test to the other. For this reason, relative permeability curves belonging to Bakken samples taken at the Court field (Figure 1), representative of the petrophysical characteristics of Facies 2, were used in the model. Results were encouraging but water production behavior at several locations could not be satisfactorily explained. Recently, relative permeability studies corresponding to poor reservoir facies with Smiley Buffalo rock and fluid samples were conducted. These studies showed extremely low relative permeability to water. This was not unexpected because Bakken samples of the Court field have displayed the same behavior. Figure 25 shows the oil-water relative permeability curves representing the good and poor rock qualities which were used in the reservoir simulation. Figure 26 show the gas-oil relative permeability curves.

Semi-permeable diaphragm air-brine capillary pressure information for different rock types was also available. For samples with flow zone indicator FZI greater than 3, where $FZI = 0.0314\ (k/\phi)^{1/2} / (\phi/(1-\phi))$, capillary pressure behavior is similar (Figure 27). For poorer rock types at least one additional capillary pressure curve is necessary. Therefore, two rock types were considered in the simulation model. Figures 28 and 29 show the original facies distribution in the sector 15-32-25W3M to 24-32-25W3M and the corresponding rock types. Facies 2 was made a single rock type and the other facies were grouped in the second rock type. The irreducible water saturations of the oil-water relative permeability curves were shifted to match the averages determined by well log analysis for each rock type. Swi = 0.24 was used for Facies 2 and Swi = 0.34 for the rest of the reservoir facies. The capillary pressure functions were rescaled to match a 2 m transition zone determined in the Bakken reservoir of Court field (Figure 1).

Production History

Production at Smiley buffalo is artificially lifted by rod pumps and progressing cavity pumps. Monitoring well performance via well testing provided only limited information due to limitations associated with pumping wells. Currently, static reservoir pressures are obtained from measurements of fluid levels in suspended wells.

We found that effective permeability's and total mobilities commonly derived from well test data were not useful for well performance analysis. Skin factors determined by well testing are invariably negative indicating some sort of formation stimulation. Such stimulation can only be attributed to sand production. In low productivity wells, following an initial burst of sand production after completion, the usual sand rate is never higher than 0.2 m3/d. However, wells with liquid rates above 200 m^3/d have shown sand production rates up to 2 m3/d (Figure 30). From Figure 30, it can also be observed that the sand production rate history of well 11/15-14-32-25W3M correlates well with the total liquid rate.

Another relevant characteristic of production behavior in the Smiley Buffalo field is the apparent stratigraphic control on water production. Figure 31 shows injector well 05-32-32-24W3M and its neighbors. Water production rates of the wells to the North of 05-32, that is 111/09-31 and 111/12-32, correlate with the injection rate (Figure 32). On the other hand, water has not been produced at neighboring wells to the south and east, 04-32, 08-31 and 31/06-32 (Figure 33). Figure 31 shows the permeability distribution in the pattern. Limited communication exists between the injector and neighboring producers to the South and East. From oil production data and from the behavior of the gas-oil ratio, it can be inferred that

pressure support from water injection at 05-32 exists at wells in which water breakthrough has not occurred or was delayed.

Finally, water production in the field is not only waterflood related, sinkholes are also contributing some water. Producers before the start of waterflooding and wells far from injectors and behind other producers, also produce water. Deeper sinkholed areas might also be partially isolating different sections of the field but, in general, are part of the reservoir as confirmed by dye injection tests. Figure 34 shows the result of dye injection and monitoring around well 13-13-32-25W3M in mid-2005. Between this injector and producer 09-14-32-25 there is a major sinkhole zone but dye was able to cross this zone to the producer.

History Match

A commercial three-phase black oil simulator was used to history match the production and pressure information of the Bakken Reservoirs in the Smiley-Buffalo field. The liquid production and water injection rates were matched. A maximum injection pressure of 16000 kPa was allowed. As mentioned before, the water-oil contact at the sinkholes was used as a history matching parameter. In general, it was found that a -115 m tvdss contact was satisfactory. The vertical to horizontal permeability ratio was 0.1 in the poorer quality rocks.

End points of the relative permeability curves were modified but the curve shape was preserved during history matching. At the end of the matching process, the end points were a critical gas saturation of 0.01, a maximum relative permeability to gas of 0.07 for both rock types, and a maximum relative permeability to water of 0.05 in poorer quality facies. Waterflood behavior in some portions of the reservoir cannot be matched based on the permeability distribution alone, as described above. A lower maximum relative permeability to water in the poorer facies was also necessary to obtain a satisfactory match.

Negative skin factors, between -3 and -6, were applied in order to match well productivities. These negative skin factors are particularly required after water breakthrough for adequate history matching.

Good static pressure control exists everywhere in the reservoir from the drilling campaign of 1997-1998. Static pressure match during the depletion period was achieved by reducing the pore volume of the poorer facies. Pore volumes of Facies 3, 4 and 5 were multiplied by 0.6, 0.25 and 0.1, respectively. Pressure match during waterflooding requires high transmissibility multipliers (up to 5 times). This permeability modification is attributed to the positive impact of sand production. The variation of permeability with time is evident from the high injectivities of old producers, the behavior of the gas-oil ratio, and low static pressures.

Figures 35 and 36 show examples of history matched wells in Sections 15-32-25 to 24-32-25W3M. Minor modifications to the reservoir information was required to reach these history match results which demonstrates the benefit of building 3D facies and property modeling for history matching Smiley Buffalo. After history matching the model, different cross-sections were analyzed in order to explain the waterflooding behavior. Figure 37 shows a West to East cross-section with the facies distribution between wells 6-15 and 8-15 in pattern 08-15-32-25W3M. Water injection at well 08-15 has been ongoing since 1998. Figure 38 shows only those grid blocks in the same cross-section where water saturation is higher than irreducible by June 2004. This occurs mainly in grid blocks in which there is higher quality facies (Facies 2), shown in dark blue. Water flows faster through Facies 2 from sinkholed areas to 6-15 and from 8-15 to 7-15. It can be concluded that the poorer quality facies are acting as partial barriers to the flow of water. The same behavior is observed in a North-South cross section between wells 01-15 and 10-15-32-25W3M.

Conclusion

A clear and concise geological model is the first step in any modelling/flow simulation project. Core logging and facies identification is an important piece as it provides the foundation of the model. It was concluded at Smiley that only those facies which are within the resolution of petrophysical logs can accurately be modelled. If a given facies type is not resolvable with conventional wireline logging, than it is nearly impossible to predict it in wells without any core data. Fortunately, the reservoir facies (Facies 2) is very resolvable and a good correlation could be made with petrophysical logs. In contrast, Facies 3 and 4 can be differentiated from Facies 2 but in a lot of cases could not be differentiated between each other. Due to time constraints, once the algorithm was accurately predicting the “reservoir facies” at Smiley Buffalo, the decision was made to move on to the statistical modelling as this would be the focus of the project. However, the importance of carefully evaluating the results of this correlation/prediction step must be stressed as it will form the foundation of all subsequent modelling and flow simulation work.

A sound geostatistical model is necessary for prediction of reservoir performance. Caution must be exercised when constructing the structural model as too much information can obscure important features or imbed anomalies. Trends are useful tools for imparting secondary information or deterministic information, but can be difficult to discern. If a trend is not clear or is inconsistent, it may be best to avoid using one. Obtaining a good static property model is often an iterative affair in conjunction with flow simulation. Over time and many iterations, the geocellular model and flow simulation become a very powerful predictive tool.

The complexity of the three dimensional facies and property modelling in the flow simulation at Smiley Buffalo is reflected in the amount of modifications necessary to reach a history match. Things such as the oil-water contact in sinkholed areas within clearly defined limits (LKO and the only contact detected by well logs), relative permeability end points of Facies 2 (which groups several facies), vertical to horizontal permeability ratios of the same rock type, and negative skin

factor to account for stimulation due to sand production all required modifying to obtain a history match. The use of detailed facies descriptions helped to understand the effect of rock-fluid interactions in waterflood performance. The latter had an immediate impact on the evaluation of injection and infill drilling decisions.

The excellent results obtained in the history matching process of Section 15 justified the generation of additional property modelling and simulation in order to achieve similar results in other areas of the field. Arithmetic upscaling of permeability properly matched the well flow capacity but tends to calculate rather high permeability's in the lower range of the permeability distribution. Geometric upscaling resulted in a permeability distribution more similar to the fine model permeability distribution in the low range. The impact of this upscaling limitation on the reservoir model has not been studied. Instead, multipliers were applied to reduce the permeability where it was deemed necessary. Application of better upscaling procedures and methods to rigorously model the permeability in the vertical direction will increase the confidence in the reservoir model. The quality of the history match in several areas presented problems associated to inadequate handling of the permeability variation due to sand production as water rate increased. Therefore, the gas-oil ratio and pressure match was negatively affected in several wells.

There appears to be a preferential flow in a SW-NE direction which might be attributed to inaccurate facies representation, natural fractures associated to sinkhole deformation, or wormholes. A reservoir simulator including petrophysical property changes as a function of sand production is thought to be necessary to match those problem areas.

Results of this work are currently being incorporated into day to day operations of the field. With more iterations and more frequent data collection, it is our hope that the model and flow simulation will continue to improve and become an integral part in managing the field. It provides us with a tool to both identify locations (drilling and injection) and predict the performance of these locations. This will alleviate some of the risk of drilling into flushed zones or converting stranded injection wells. It will provide a tool that will allow the technical team to make better reservoir management decisions.

Acknowledgments

We would like to acknowledge the contribution of many people that helped get this project off and running and those who made contributions throughout the process. The Calgary staff of Dale Vanhooren *(Geophysicist)*, Allan Pickel *(Petrophysicist)*, Maureen McHenry *(Technologist)*, Joan Voytechek *(Technologist)*, Heather Rogan *(Reservoir Engineer)*, and Michael Moriarty *(Reservoir Engineer)*. Field staff of Ken Imlach *(Production Engineer)*, Ryan Craig *(Production Engineer)*, Trevor Kissick *(Lead Operator)*, and the rest of the field staff should be commended on all their work to get us the data we needed.

References

1. Kasper, D.: "Stratigraphy and Sedimentology of the Bakken Formation of West-central Saskatchewan: A Preliminary Report", *Saskatchewan Geological Survey: Summary of Investigations*, (1992).
2. Snedden, J.W. and Dalrymple, R.W.: "Modern Shelf Sand Ridges: From Historical Perspective To A Unified Hydrodynamic and Evolutionary Model", *Isolated Shallow Marine Sand Bodies: Sequence Stratigraphic Analysis and Sedimentological Interpretation, SEPM Special Publication No. 64*, (1999) 13.
3. Huthnance, J.M.: "On One Mechanism Forming Linear Sand Banks", *Estuarine, Coastal and Shelf Science,* **Vol. 14**, (1982) 79.
4. Hulscher, S.J.M.H., DeSwart, H.E. and DeVriend, H.J., "The generation of offshore tidal sand banks and sand waves", *Continental Shelf Research*, **Vol. 13**, (1993) 1183.
5. Swift, D.J.P., "Response of the shelf floor to flow", *in Tillman, R.W., Swift, D.J.P. and Walker, R.G., eds., Shelf Sands and Sandstone Reservoirs: Tulsa, Society for Sedimentary Geology) Short Course Notes 13*, (1985) 135.
6. Vanhooren, D., "Smiley Geophysics", *in Mohr, R., Smiley Buffalo Geological Overview: Petrel 3D Modelling and Future Upside Potential, Nexen Inc Internal Report,* July 2004.
7. Briggs, I., "Machine Contouring Using Minimum Curvature", *Geophysics*, **Vol. 39**, No. 1, (Feb. 1974).
8. Deutsch, C. and Journal, A., "*GSLIB"* Geostatistical *Software Library and Users Guide, second edition, Oxford University Press*, *New York*, (1998).
9. Pickel, A., "Smiley-Buffalo Petrophysical Study: Middle Bakken Formation", *Nexen Inc Internal Report*, (July 2003).
10. Mohr, R., "Smiley Buffalo Geological Overview: Petrel 3D Modelling and Future Upside Potential", *Nexen Inc Internal Report*, (July 2004).

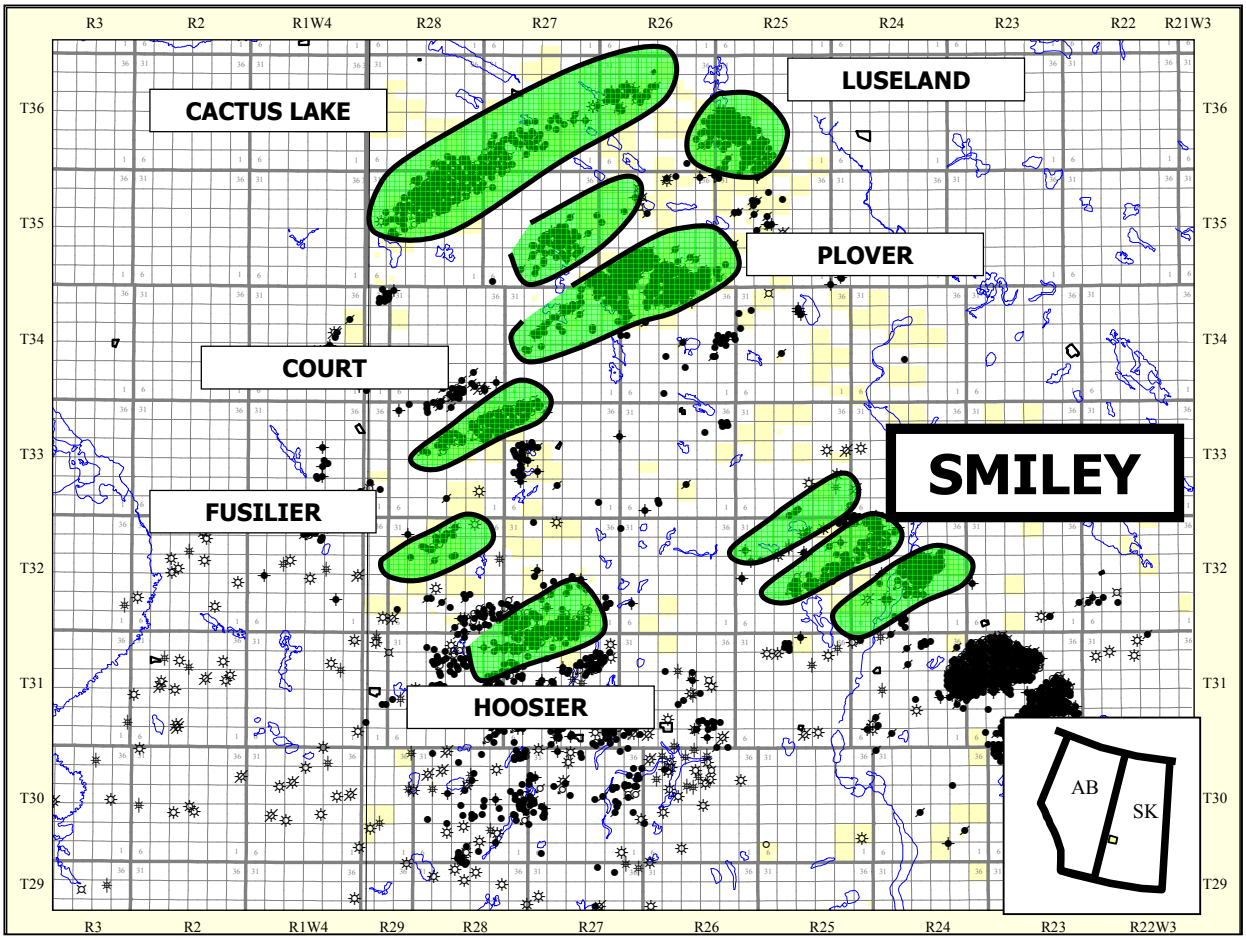

Figure 1 - Bakken Sand Ridges throughout West-Central Saskatchewan

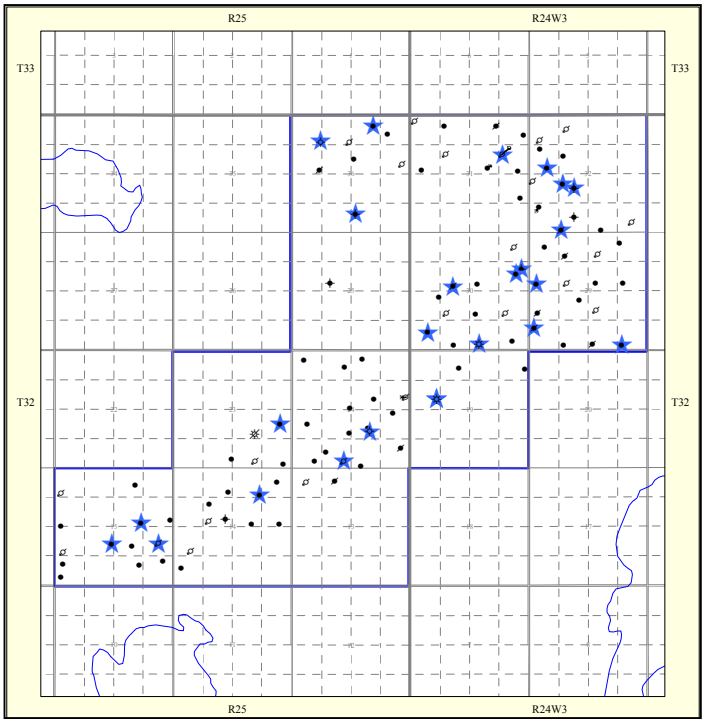

Figure 2 - Smiley Base Map. (★ Cored Wells)

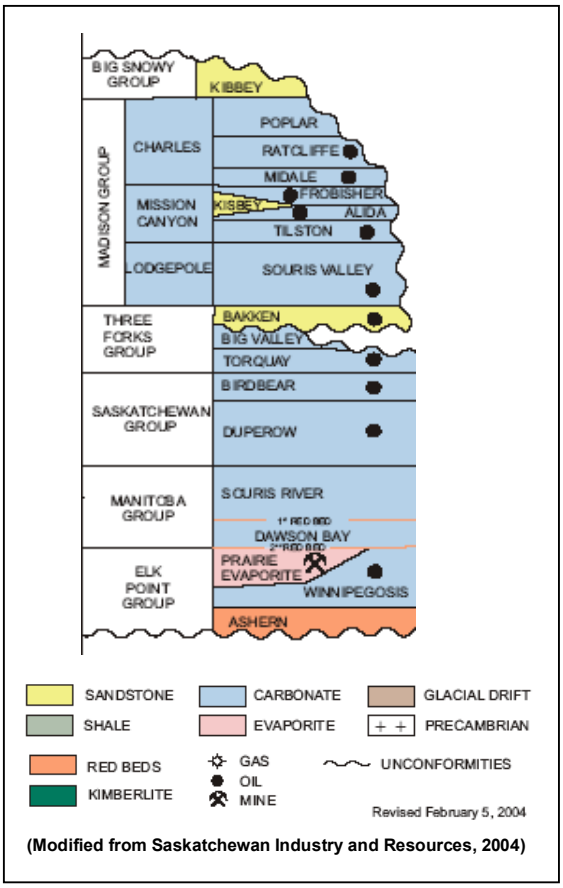

Figure 3 - Saskatchewan Stratigraphic Chart (modified from Saskatchewan Industry and Resources, 2004)

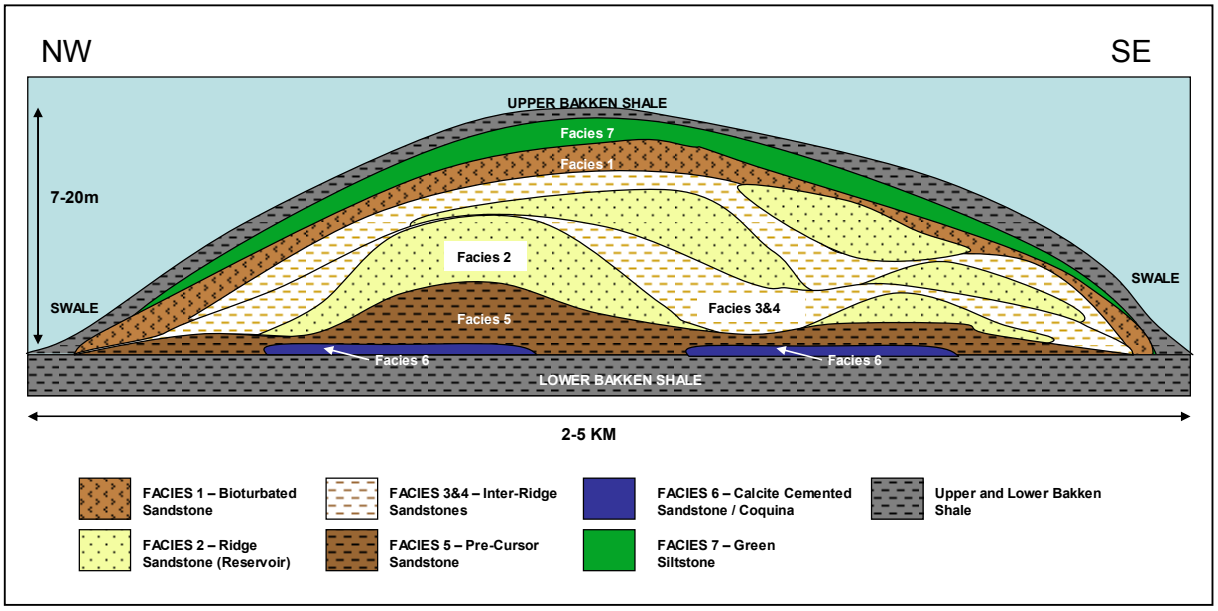

Figure 4 - Deposition Model of the Mississippian-Devonian Bakken Formation in West-Central Saskatchewan

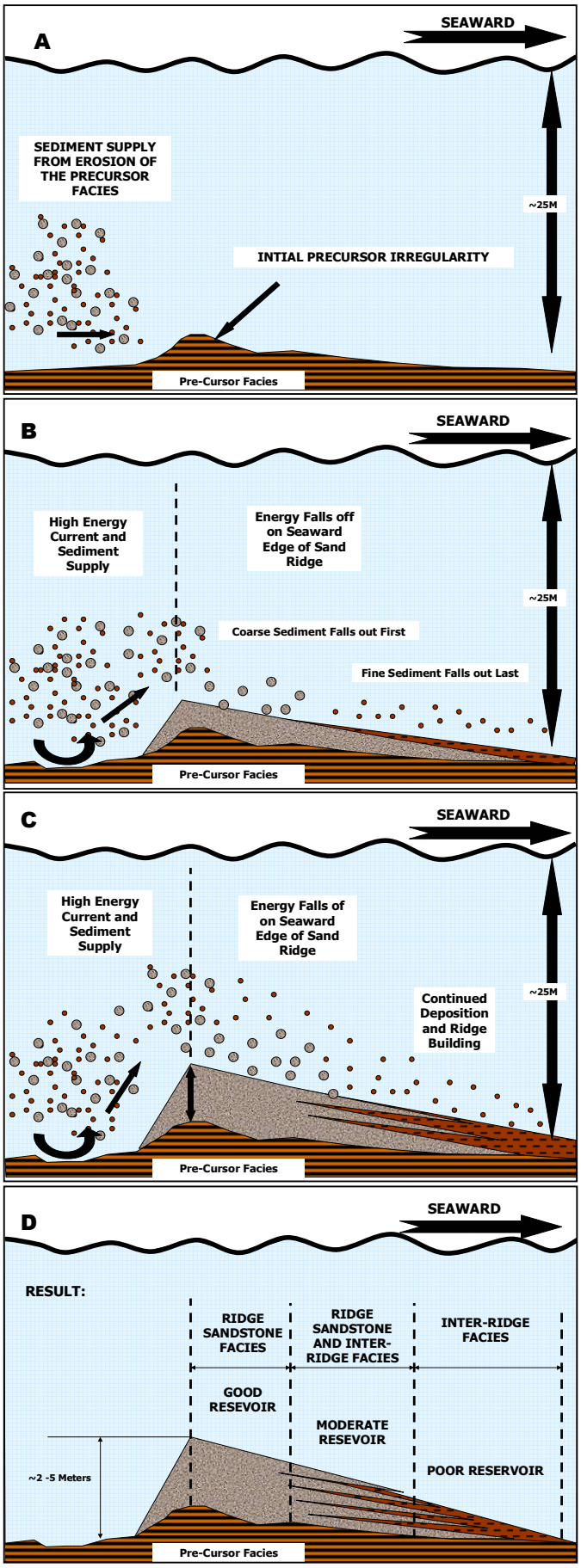

Figure 5 - Depositional Process of a Single Ridge (Reservoir) Sand[10]

(A) An initial pre-cursor irregularity exists which provides the nucleation point for ridge formation.

(B) Shoreline currents erode the precursor shelf facies, put sediment into suspension, and then redeposit it further down current. As currents hit the landward side of the irregularity, energy drops off allowing course sediment to fall out first and fine sediment to fall out further seaward.

(C) Ridge Growth continues and they build upward and migrate in a seaward direction.

(D) In each individual ridge unit, the best reservoir will be located immediately seaward of the apex of the ridge, getting progressively worse as you move in a seaward direction.

It must be stressed that this diagram illustrates the development of a single ridge sand. As deposition continues, ridge sands will be stacked on as long as there is a continued supply of sediment into the system. In core, as many as 5 ridge events can be interpreted in the middle Bakken at the study area.

Figure 6 - Facies Breakdown for the Middle Bakken Reservoir at Smiley Buffalo. 7 facies types were defined and modelled throughout the study area.

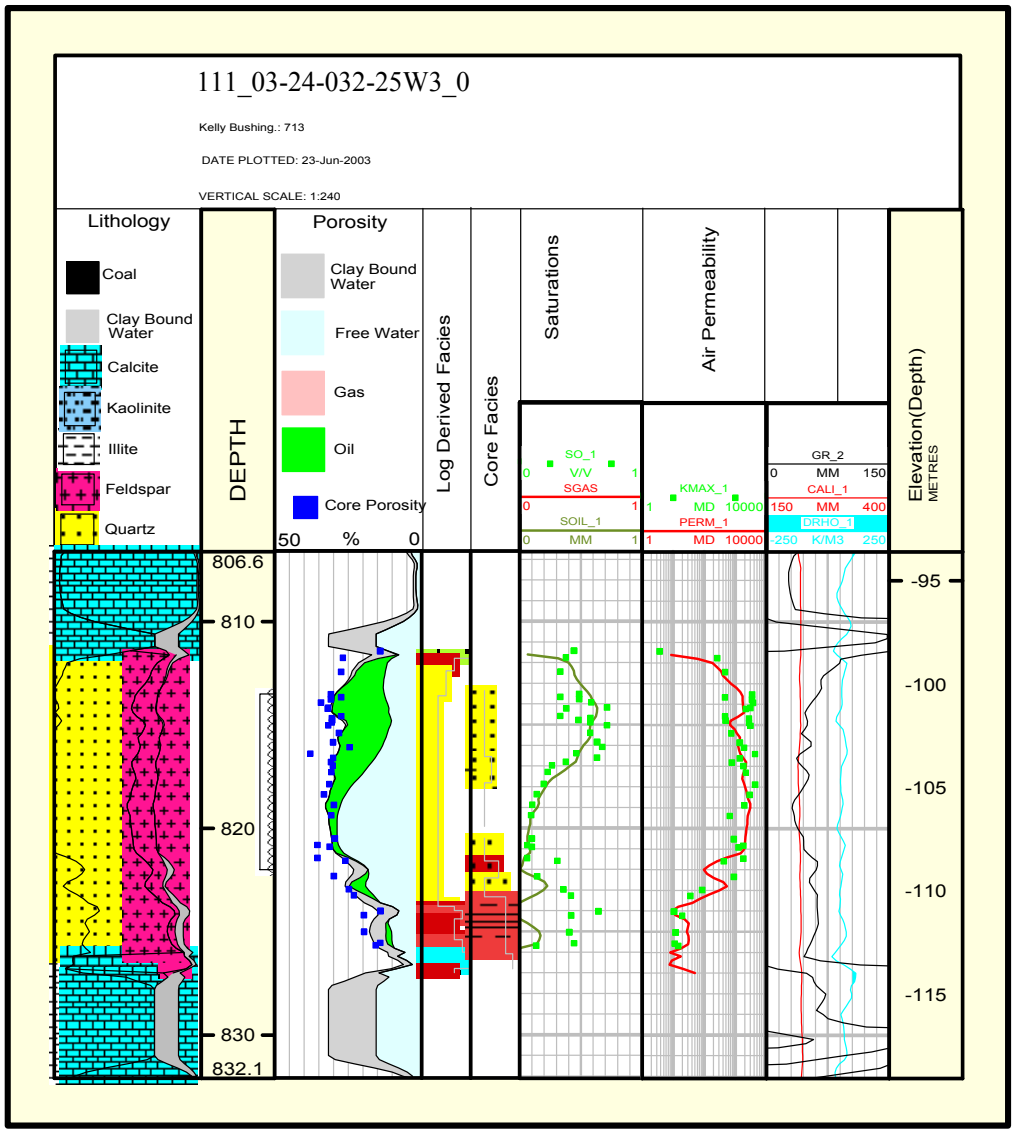

Figure 7 - Example Log from a cored well at Smiley. A comparison is shown in tracks 4&5 of log derived facies vs. actual core facies. A fairly consistent match was obtained in this well.

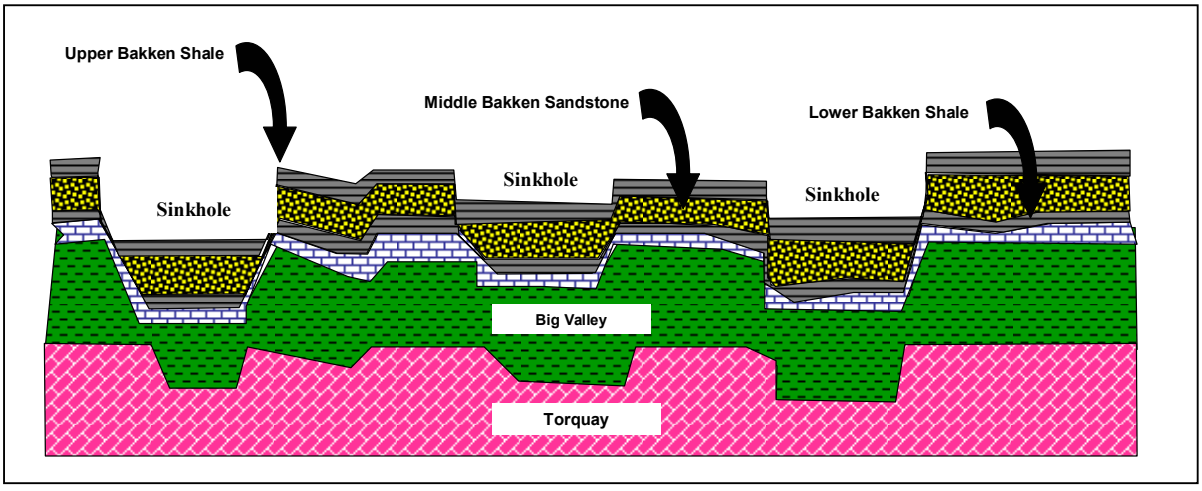

Figure 8 - Architecture of Sinkholes in the Bakken reservoir. This cartoon was put together to illustrate how the scale of sinkholes will determine whether communication through them is possible or not.

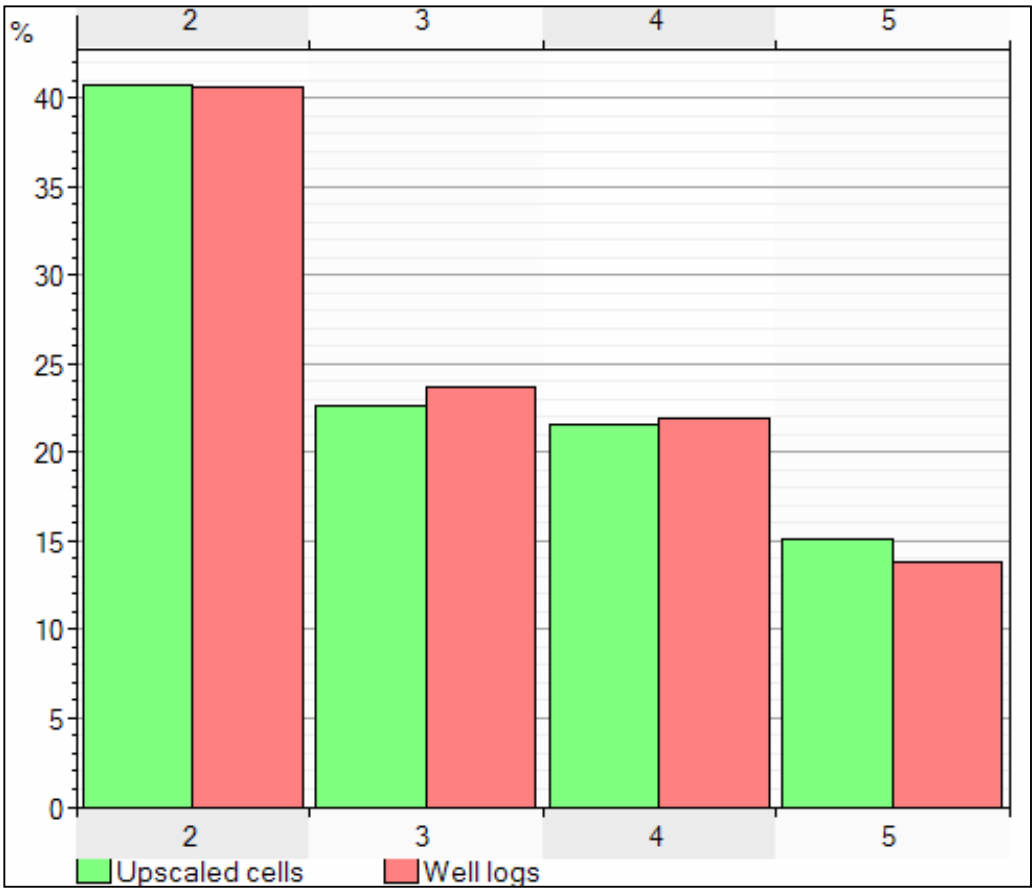

Figure 9 - The raw (right bins) and upscaled (left) facies proportions

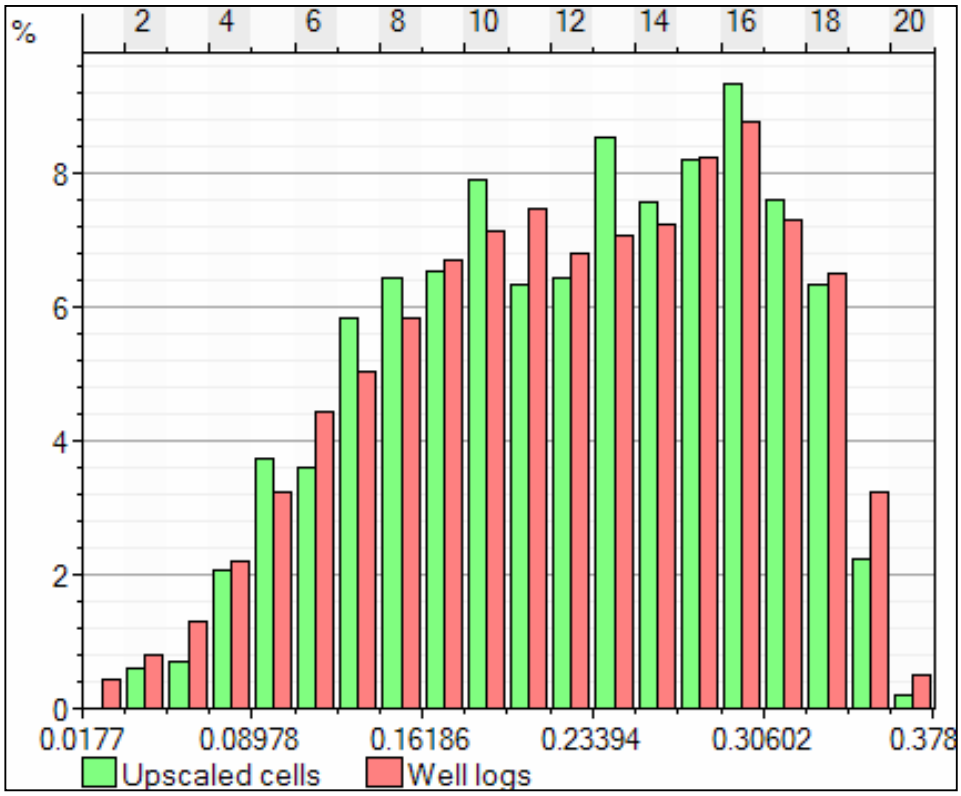

Figure 10 - the raw (left) and upscaled porosity histograms.

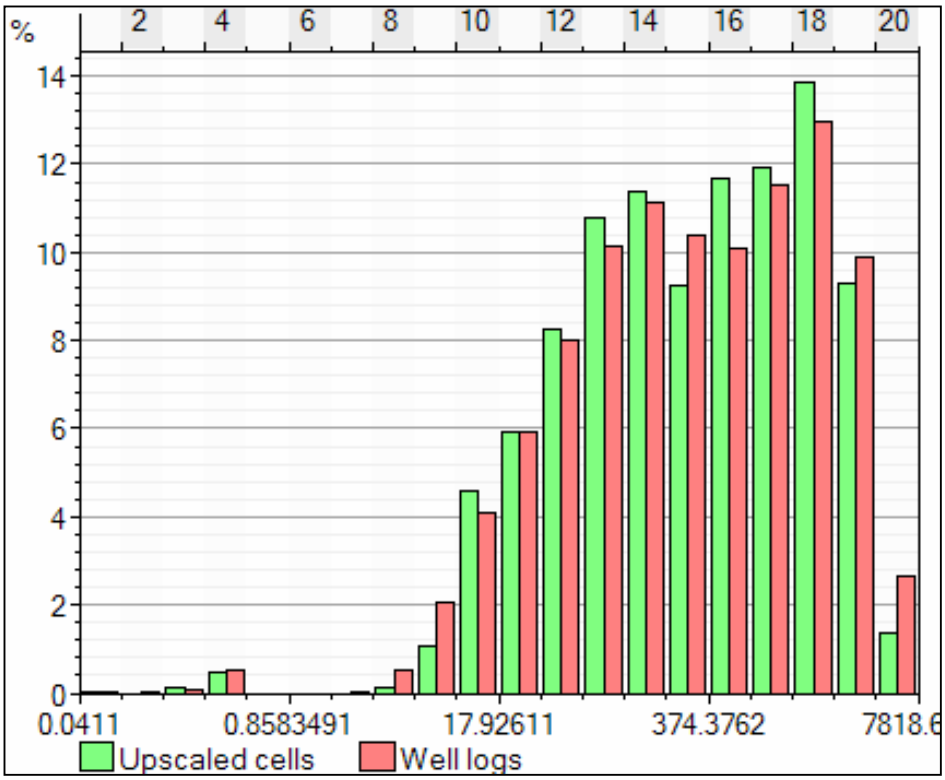

Figure 11 - the raw (left) and upscaled permeability histograms

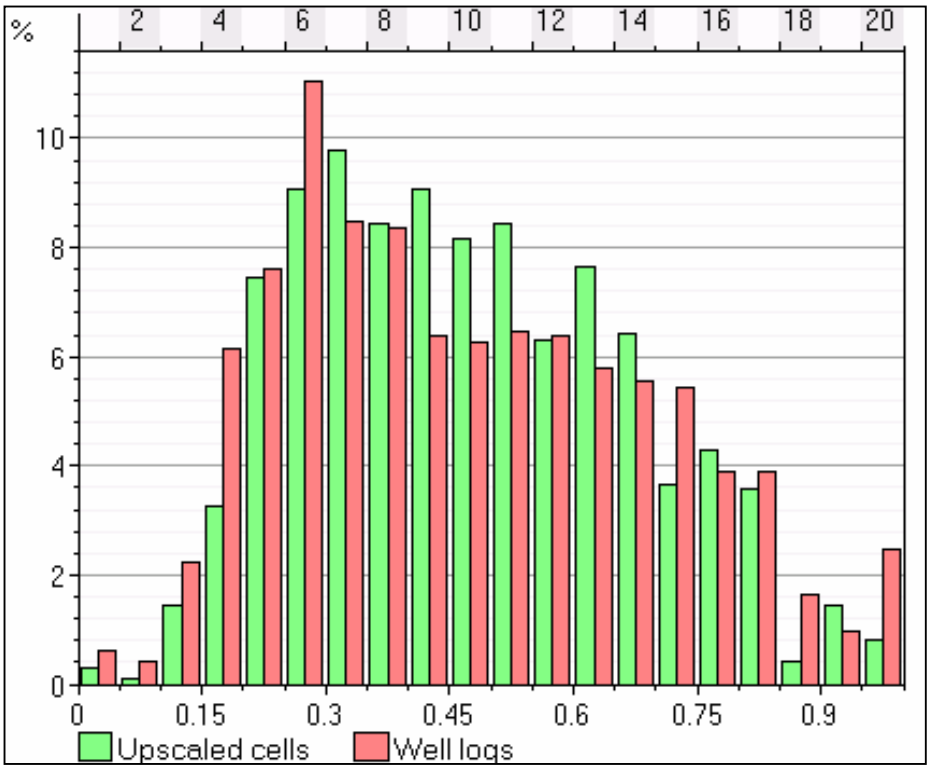

Figure 12 - the distributions of raw and upscaled water saturation. The upscaled saturations are in the left bin and the raw water saturations are in the right bins.

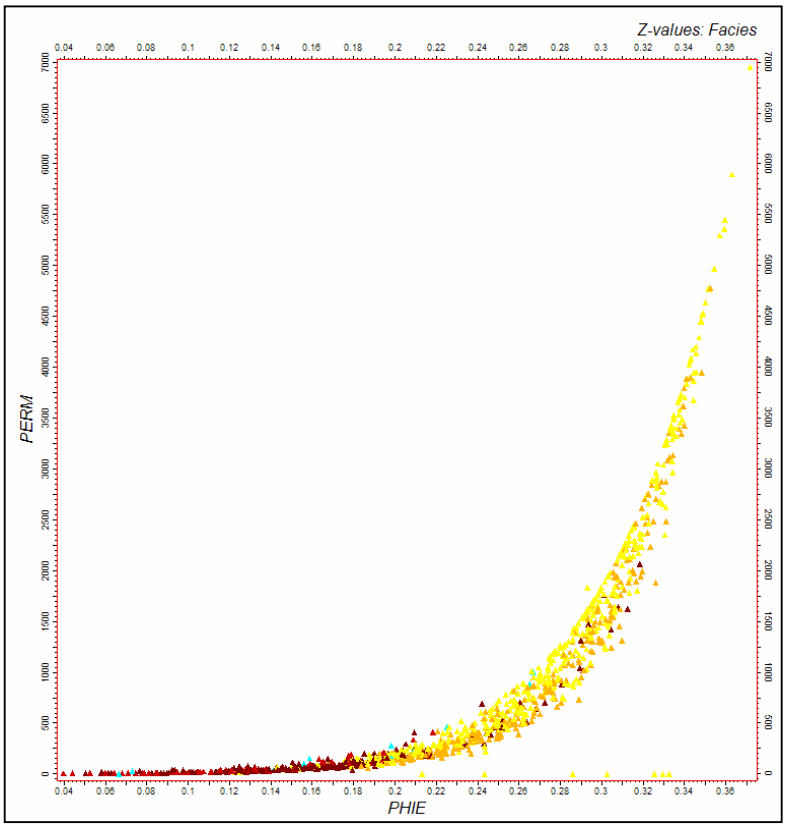

Figure 13 - A scatterplot of porosity (x-axis) and permeability (y-axis). The points are colored by facies with the darkest being Facies 4, and the lightest being Facies 2.

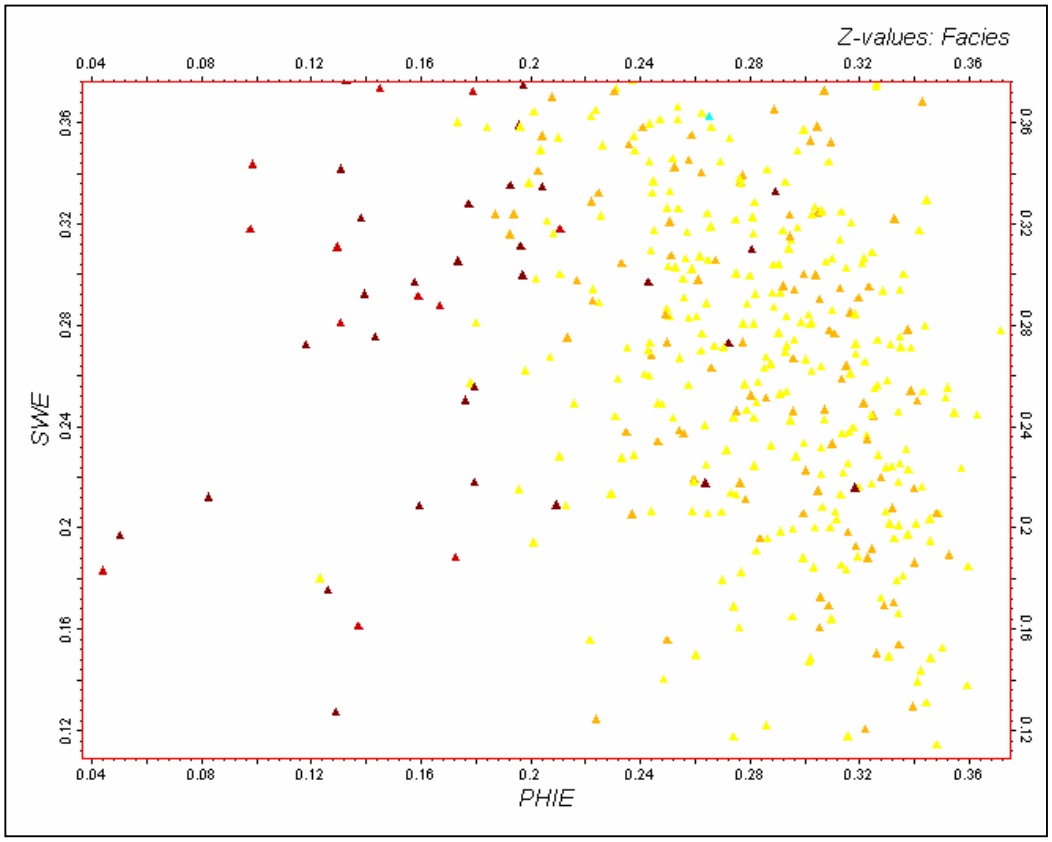

Figure 14 - A scatterplot showing porosity on the x-axis and water saturation on the y-axis. The points are colored by facies. The darkest points are for Facies 4, and the lightest are for Facies 2.

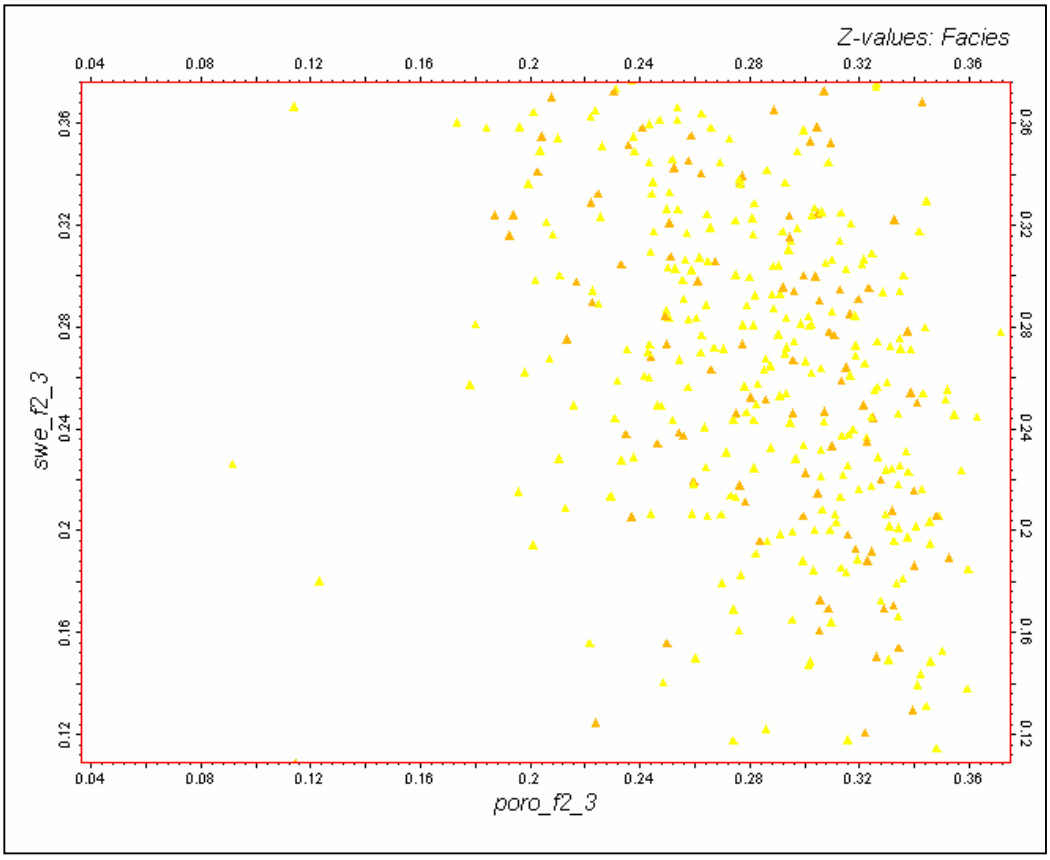

Figure 15 - a scatterplot of porosity on the x-axis and water saturation on the y-axis for Facies 2 and 3 only. The darker points are Facies 3.

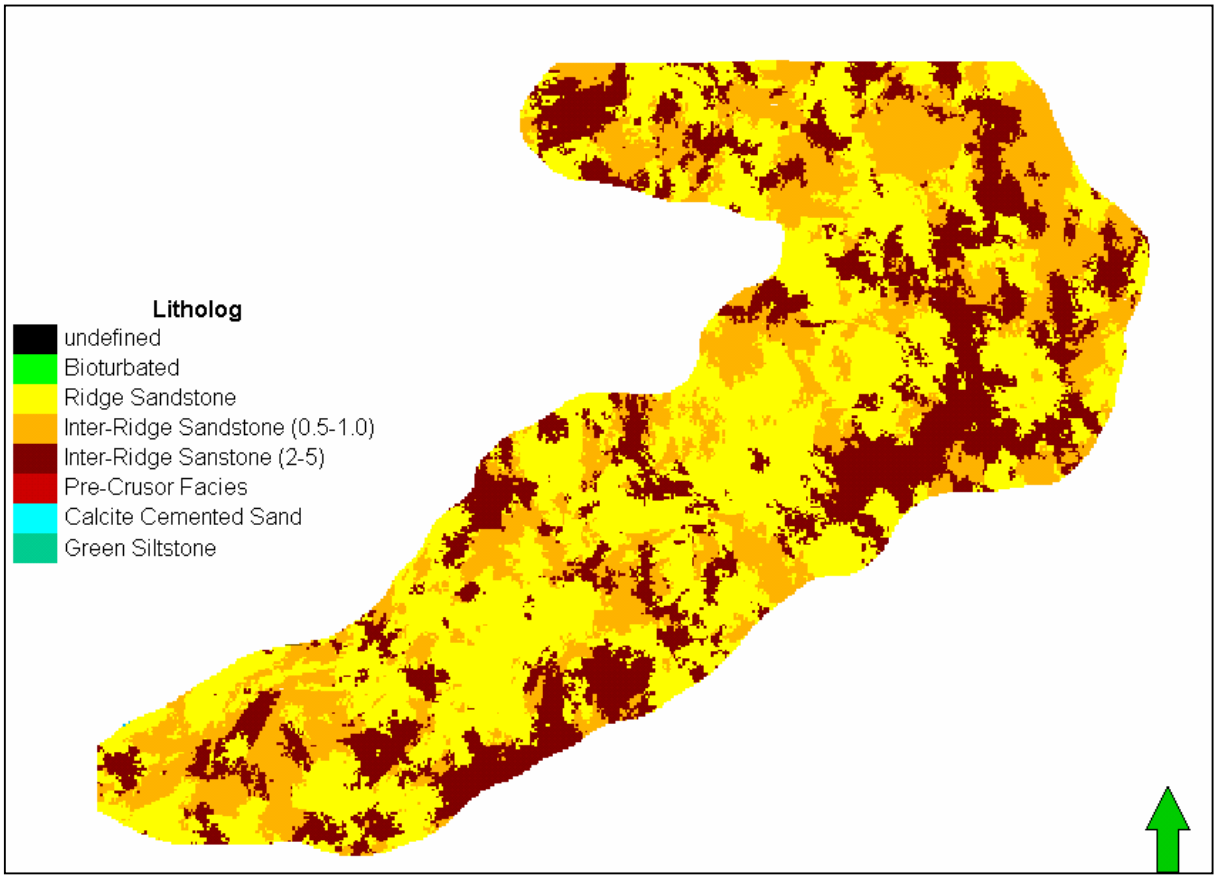

Figure 16 – Facies Distribution throughout the study area (realization 50)

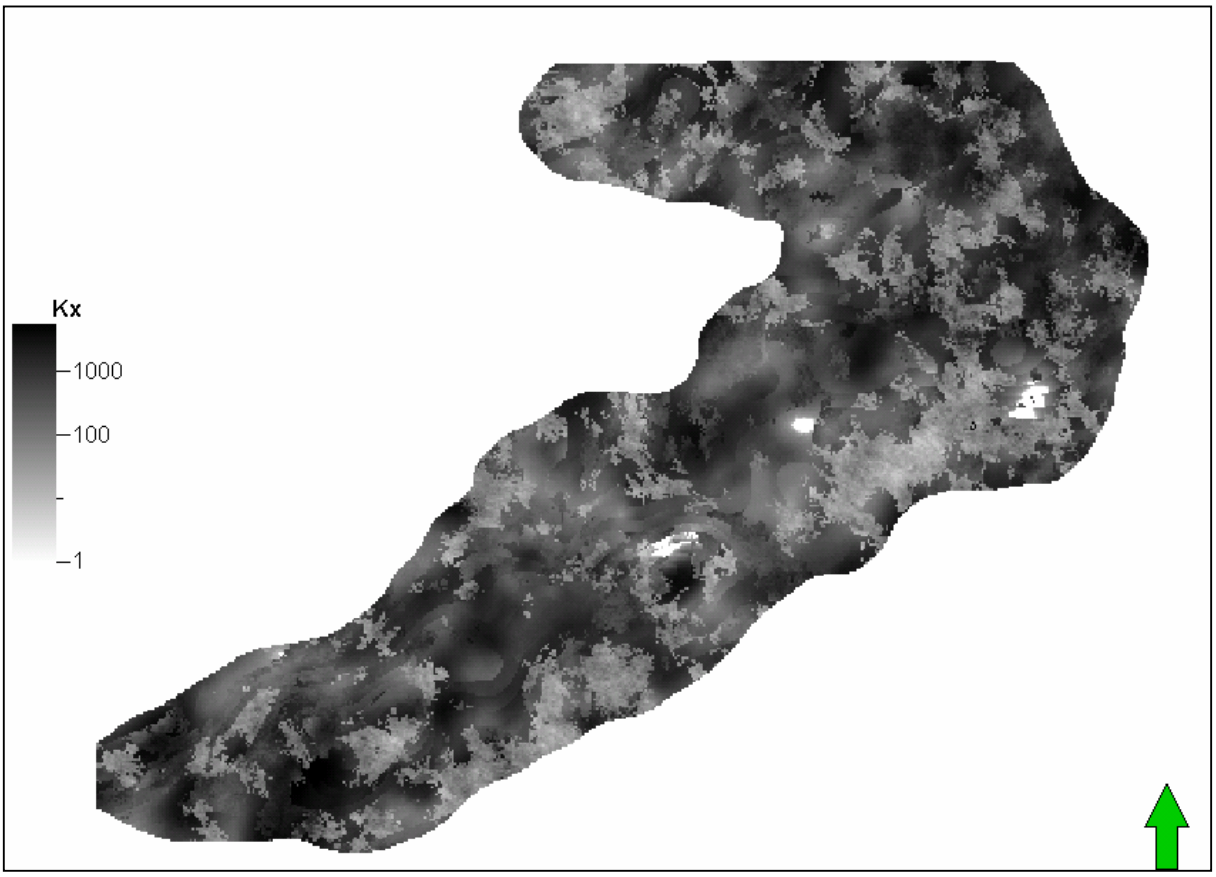

Figure 17 – Permeability Distribution throughout the study area (realization 50)

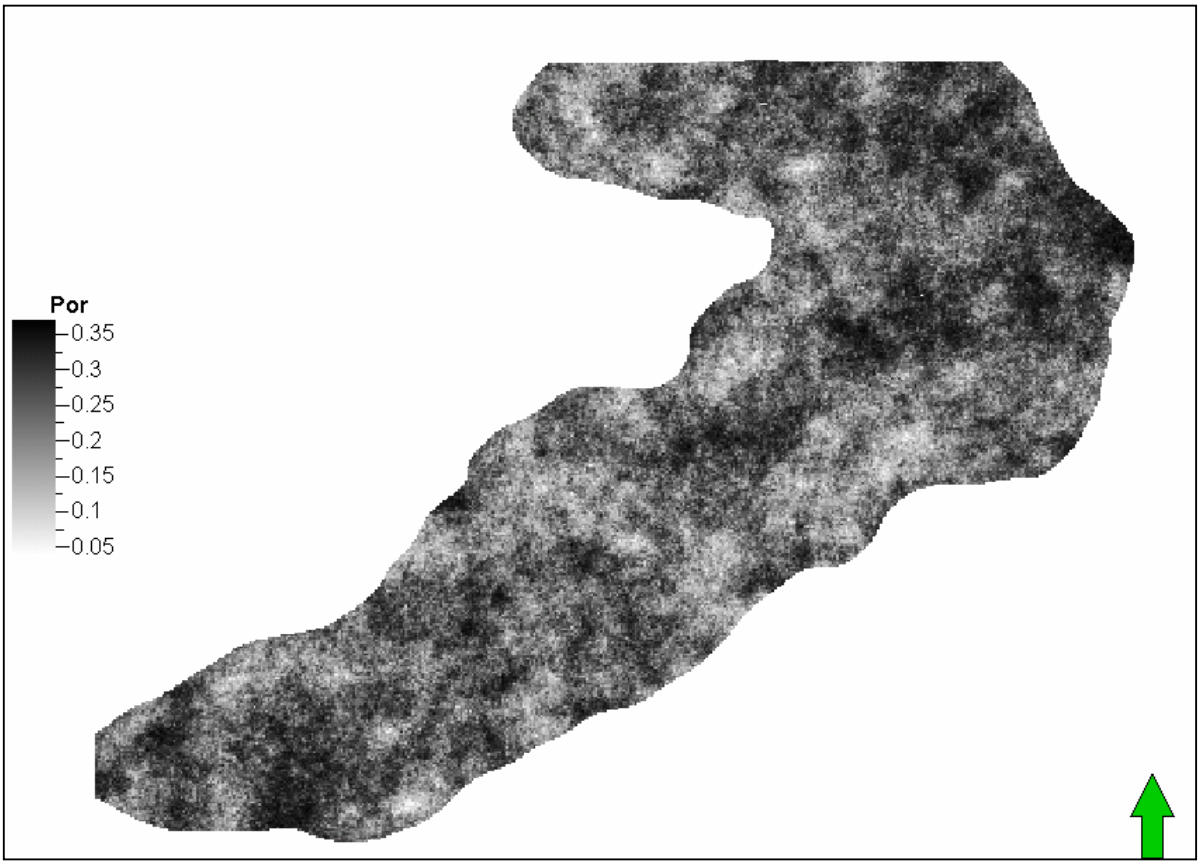

Figure 18 - Porosity Distribution throughout the Study area (realization 50)

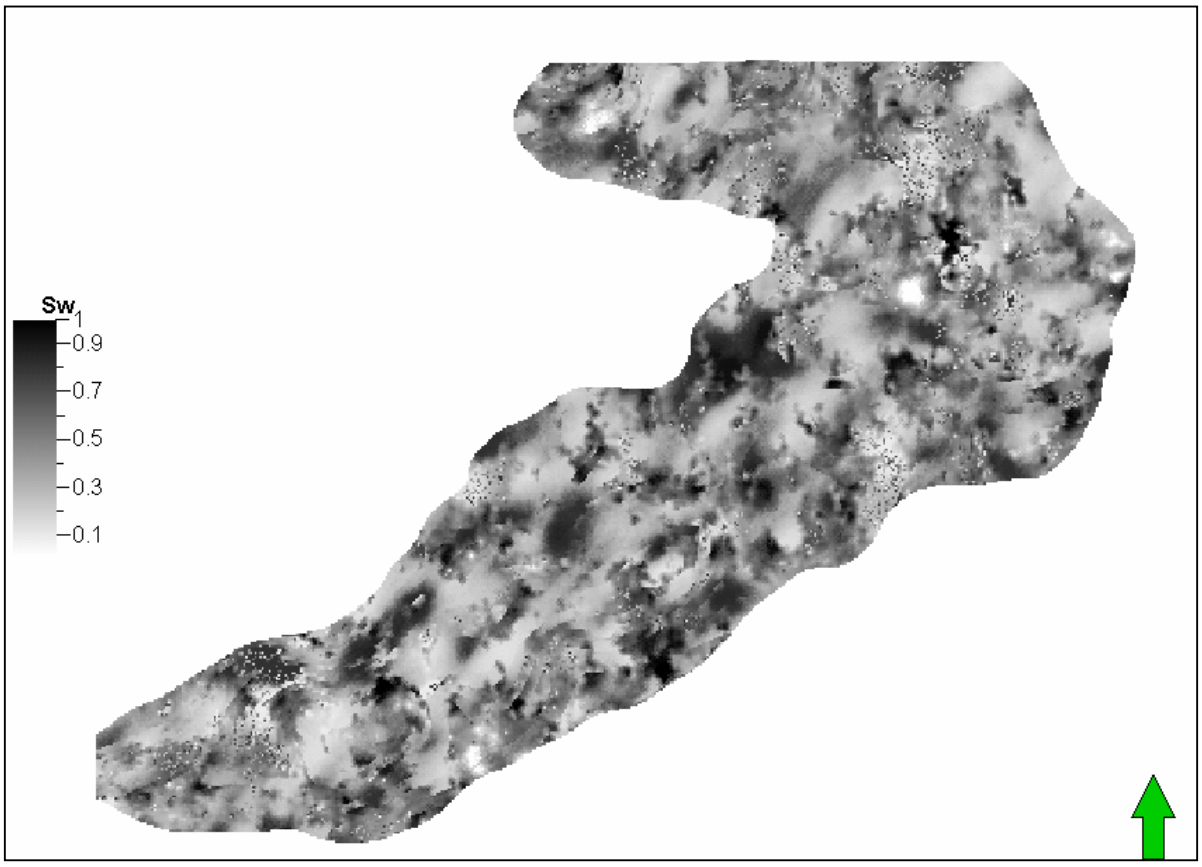

Figure 19 - Water Saturation Distribution throughout the study area (realization 50)

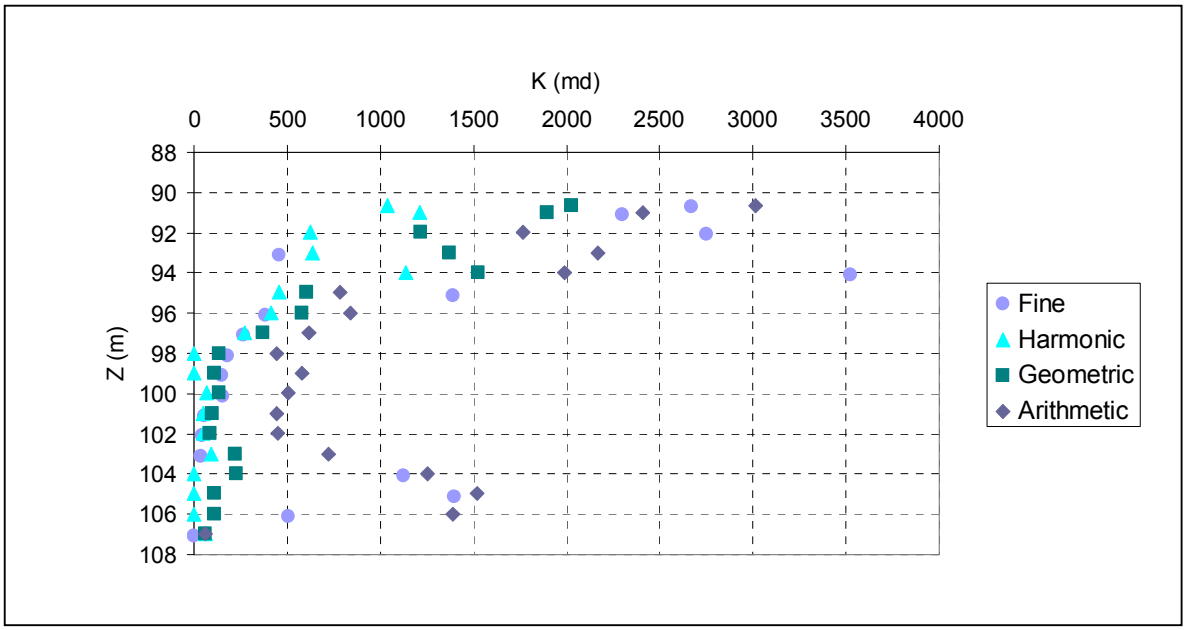

Figure 20 - 08-15-32-25W3M Permeability Profiles.

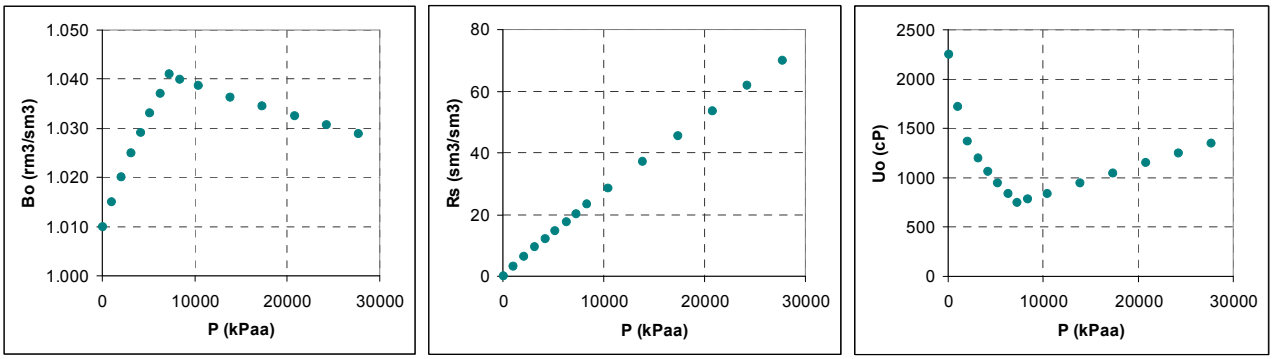

Figure 21 - Bakken Reservoir Smiley Buffalo field. Oil PVT Properties

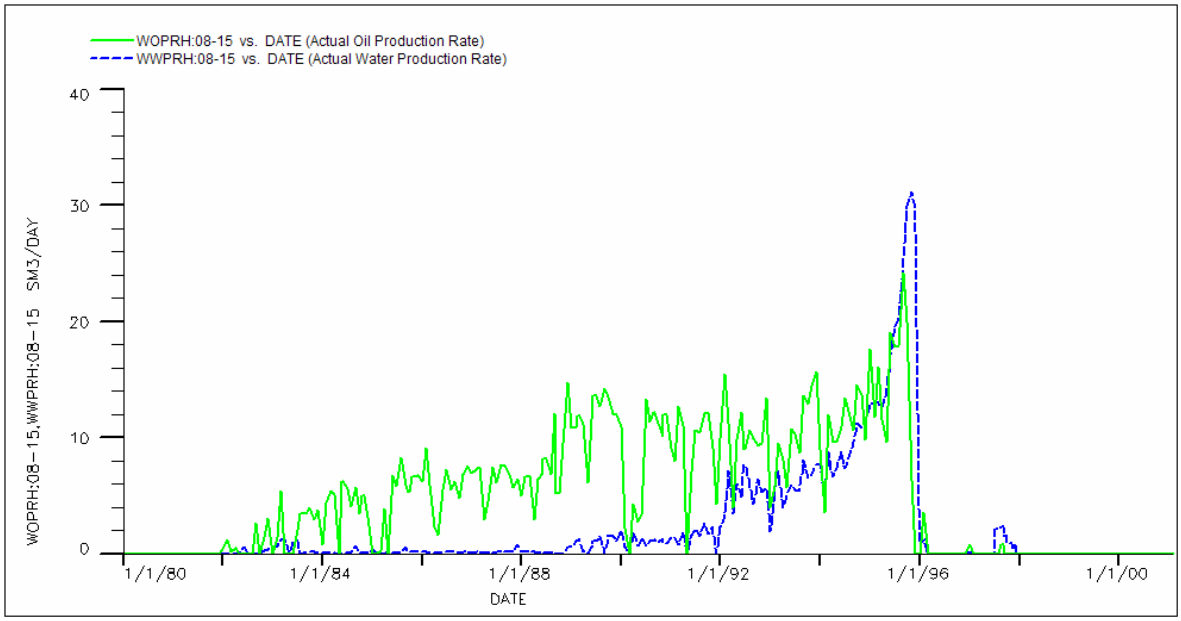

Figure 22 - Water Production Before Waterflood. 01/08-15-32-25W3M

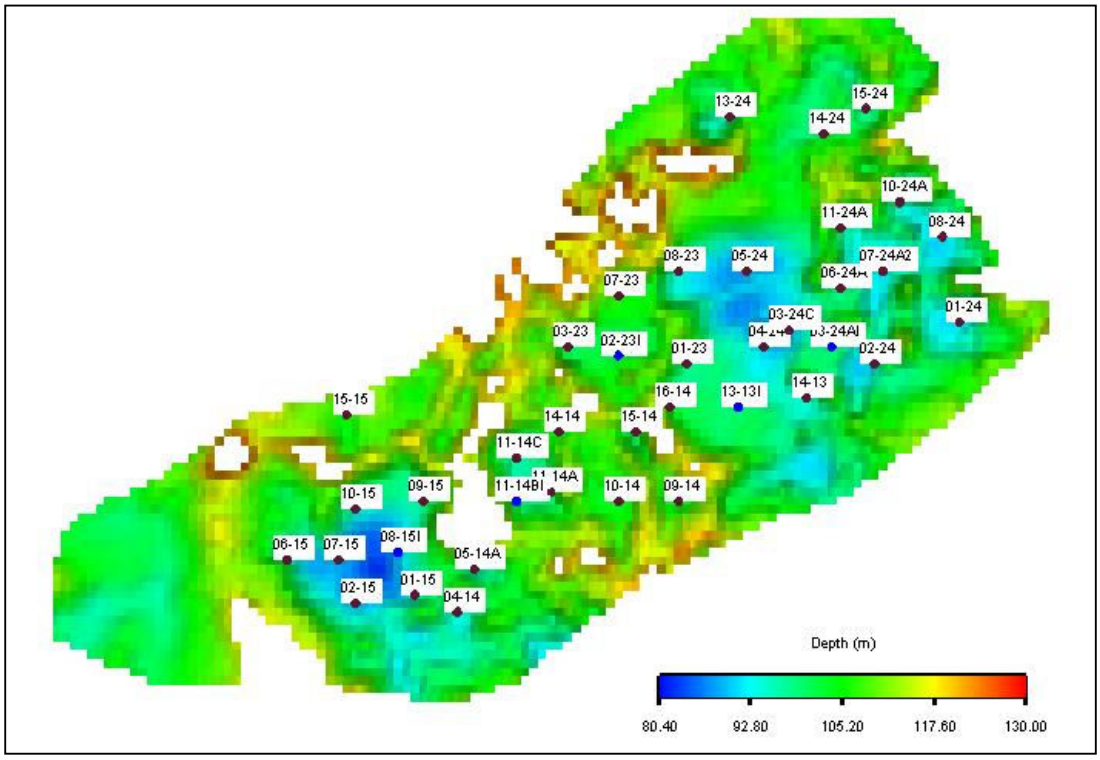

Figure 23 - Depth to Top of Bakken Reservoir. Sector 15-32-25W3M to 24- 32-25W3M

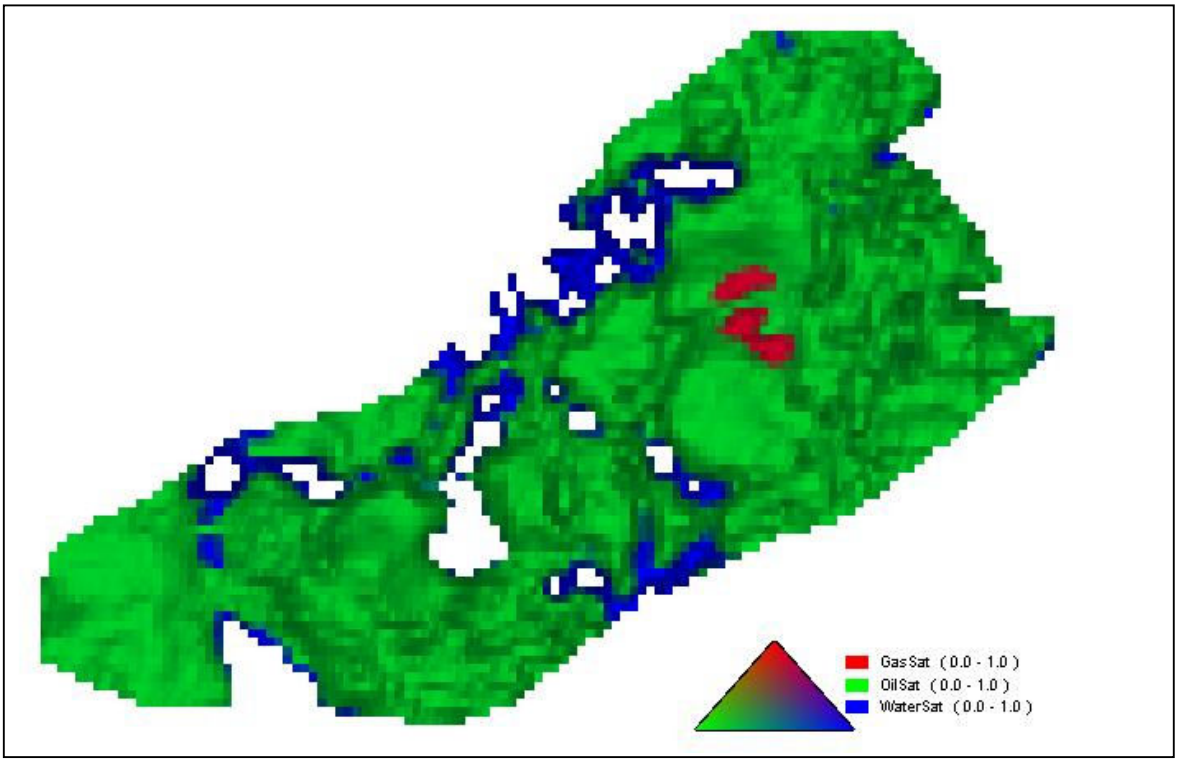

Figure 24 - Initial Fluid Contacts. Top of Bakken. Sector 15-32-25W3M to 24- 32-25W3M

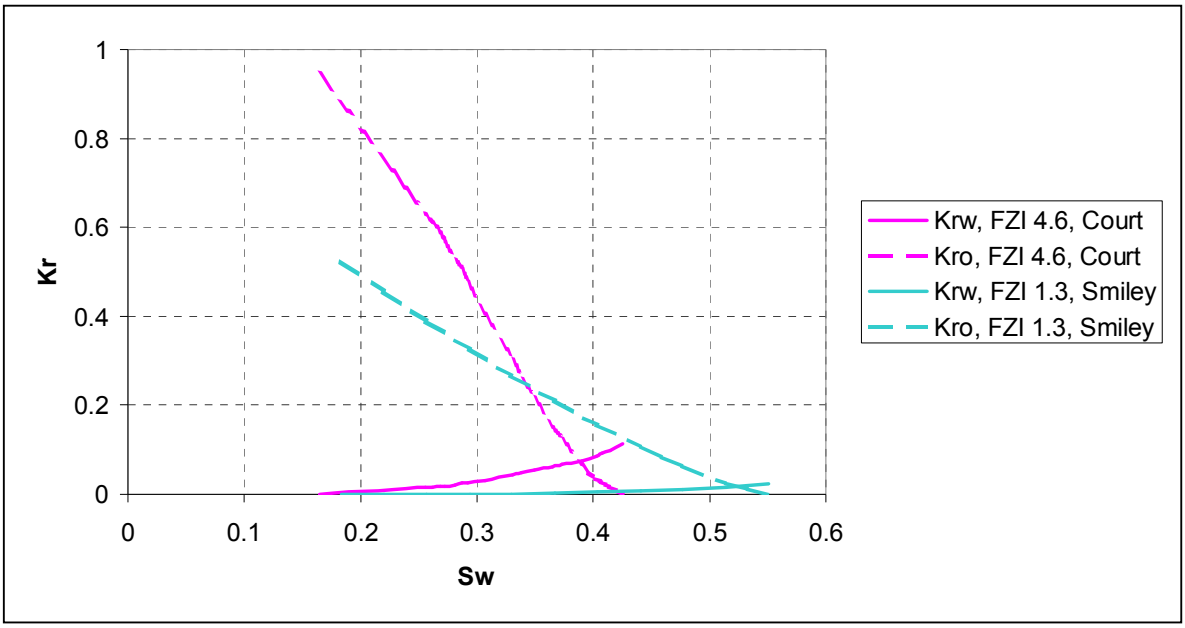

Figure 25 - Oil-Water Relative Permeability Curves. Two Rock Types.

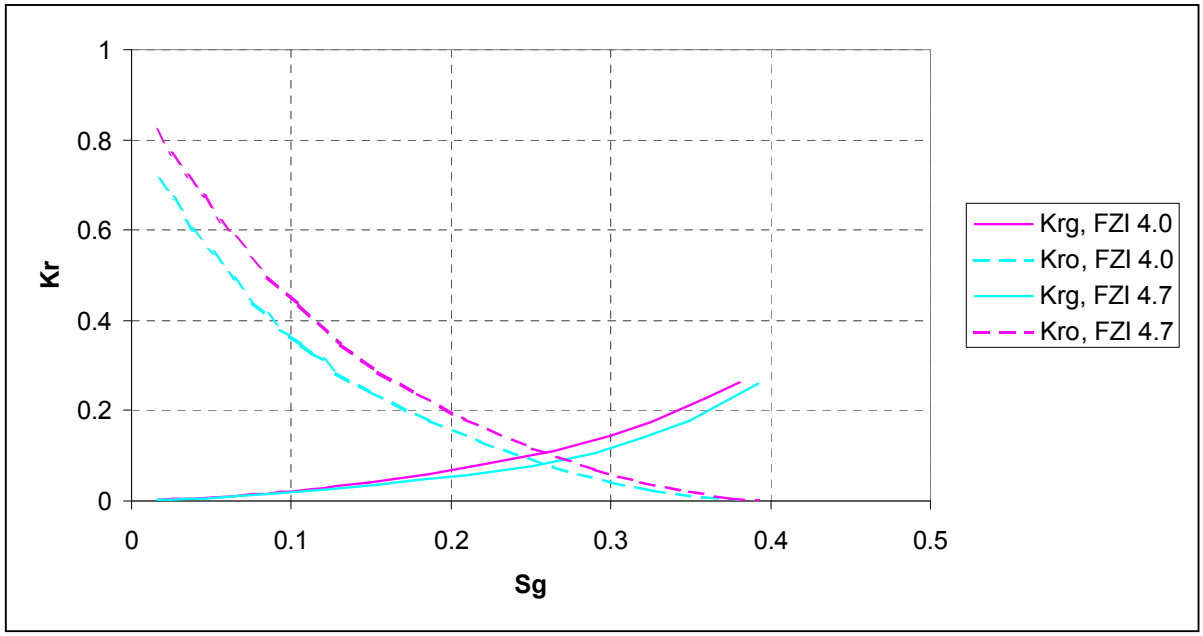

Figure 26 - Oil-Gas Relative Permeability Curves.

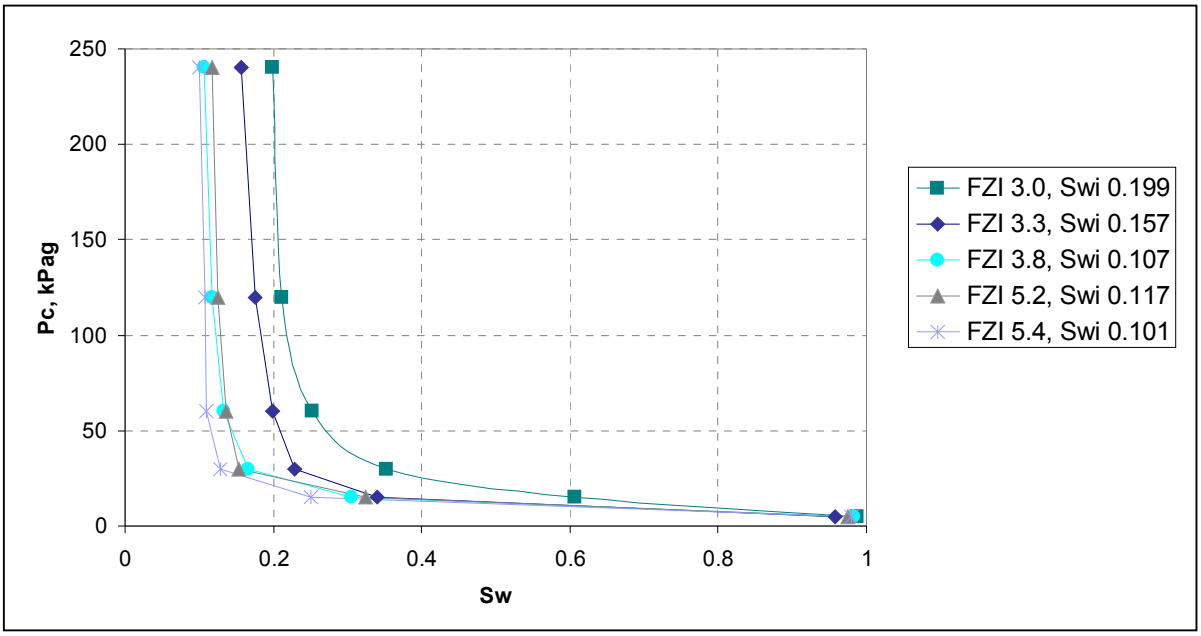

Figure 27 - Capillary Pressure Data

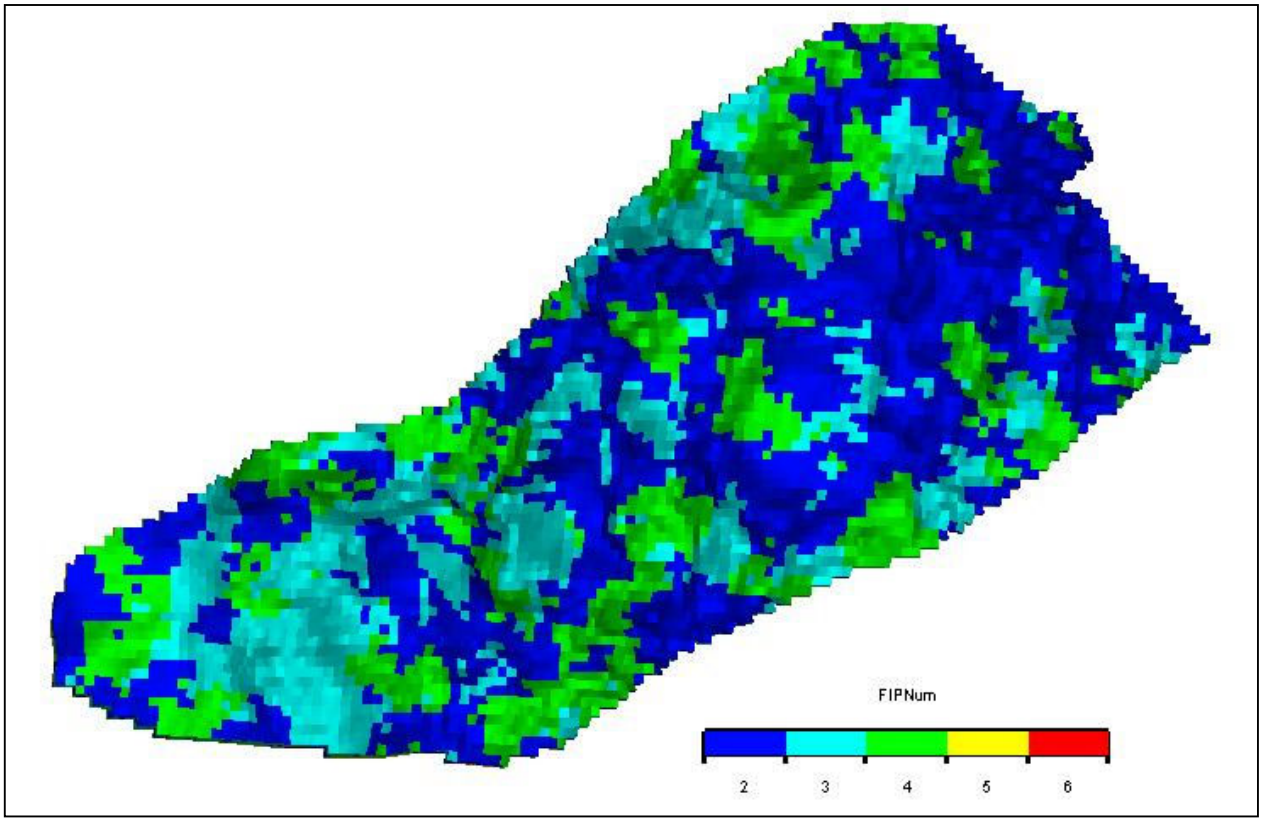

Figure 28 - Upscaled Model. Facies Distribution

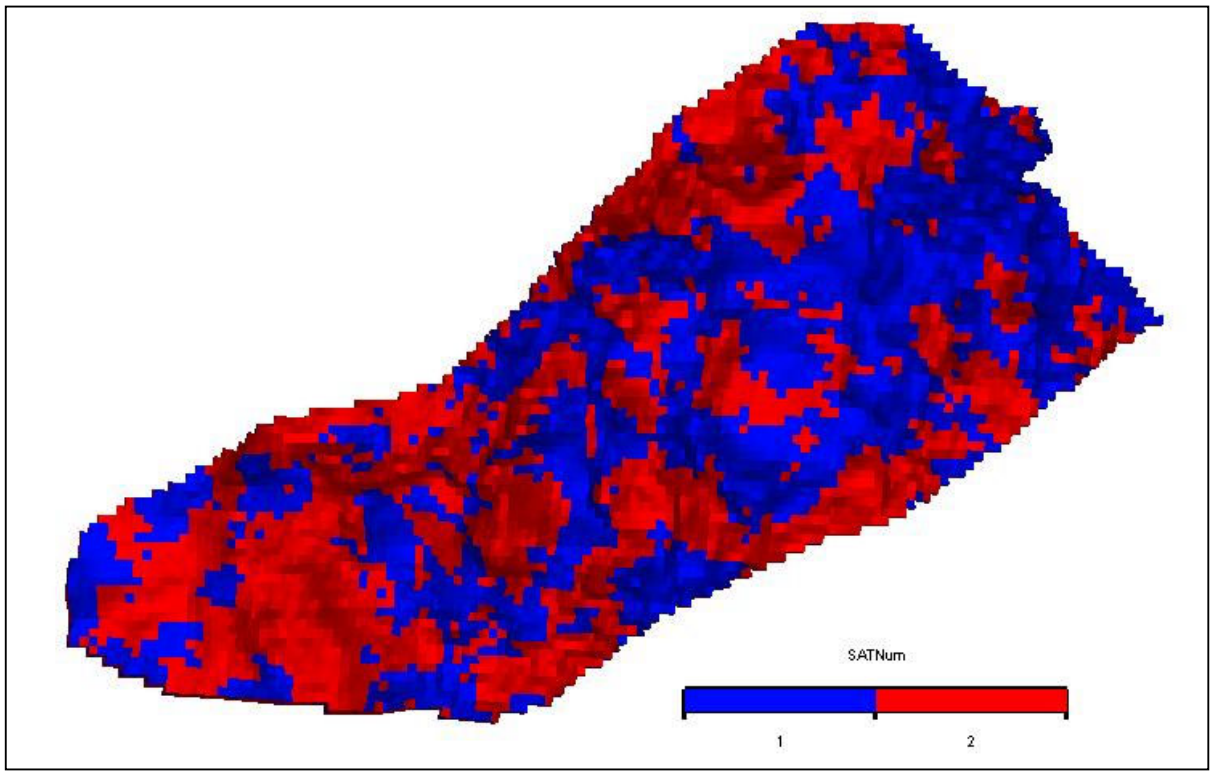

Figure 29 - Upscaled Model. Rock Types Distribution

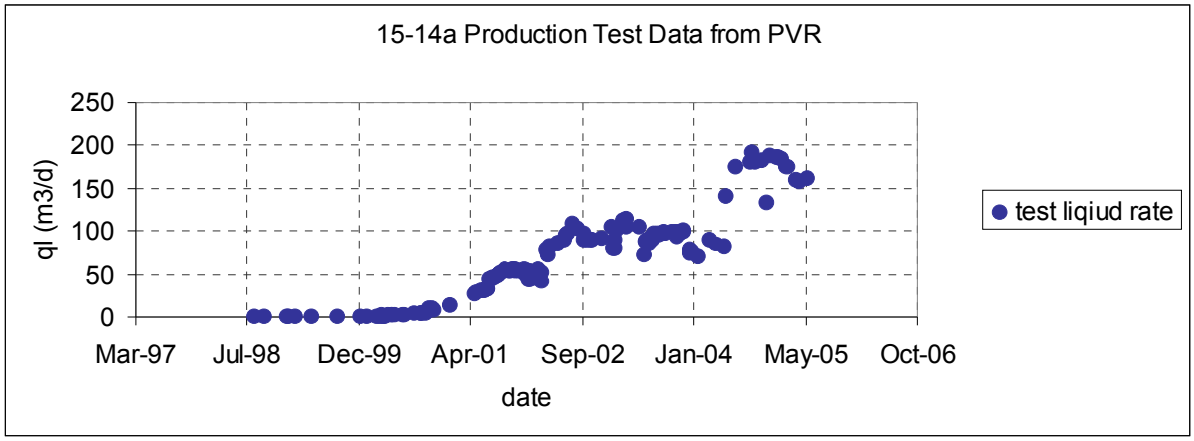

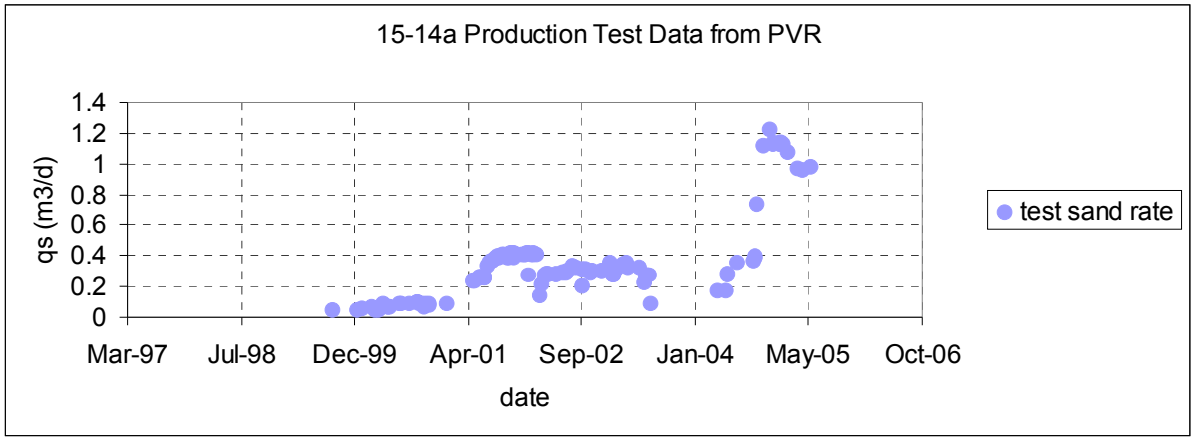

Figure 30 - Sand Rate from Production Tests. 06-15-32-25W3M

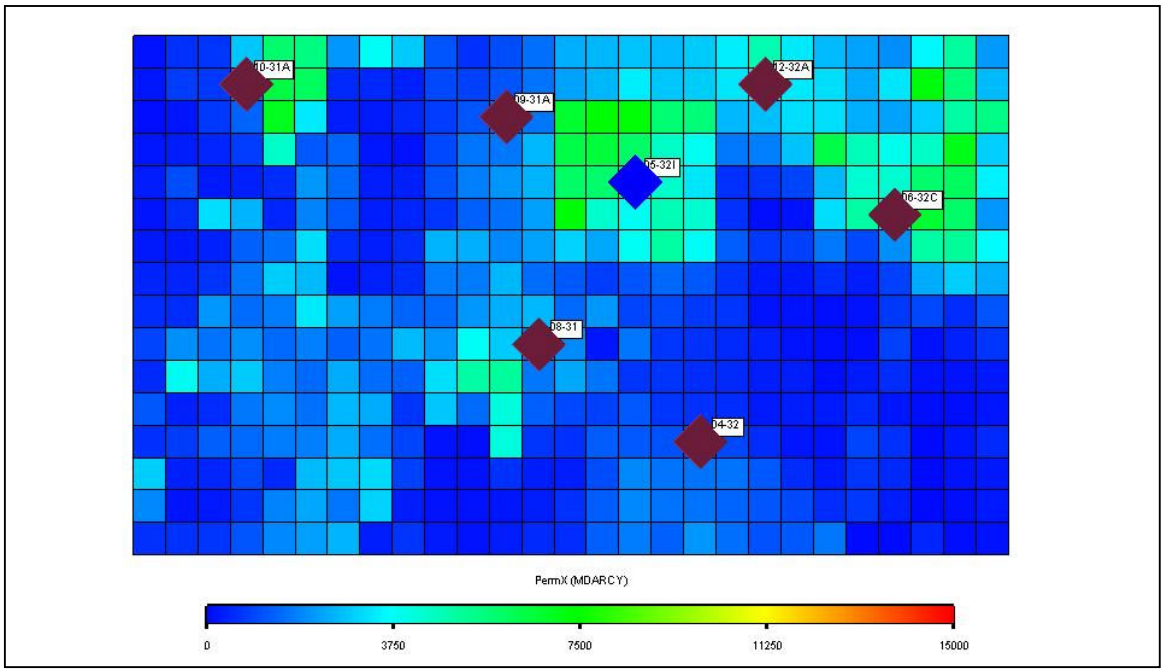

Figure 31 - Pattern 05-32-32-24W3M. Permeability Distribution

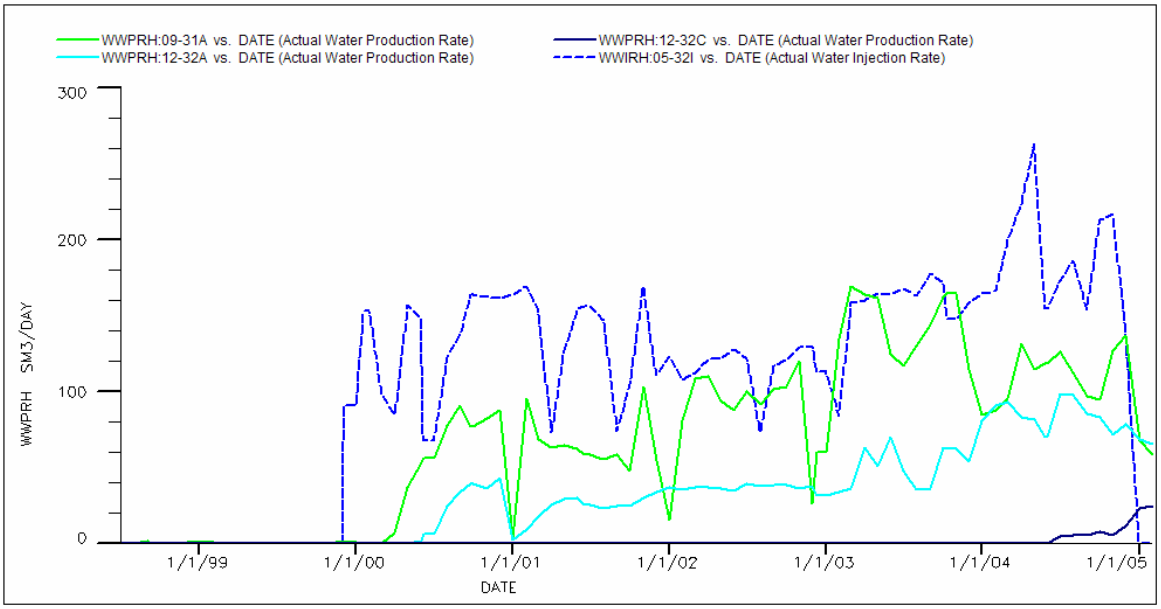

Figure 32 - Pattern 05-32-32-24W3M. Water Injection and Water Production Rates. Northern Wells

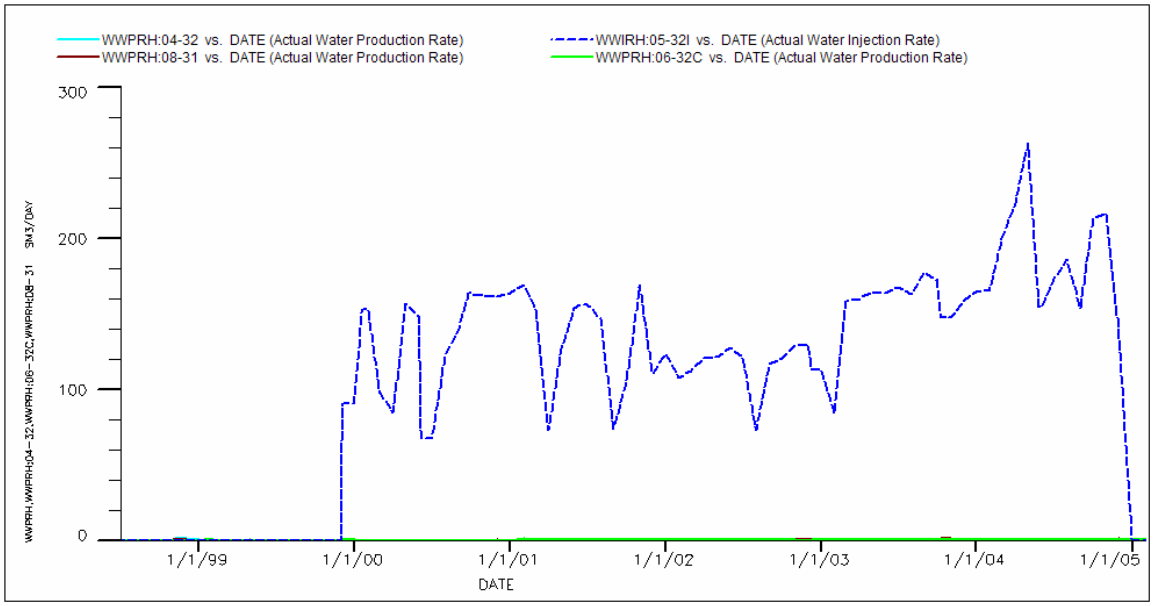

Figure 33 - Pattern 05-32-32-24W3M. Water Injection and Water Production Rates. South and East Wells.

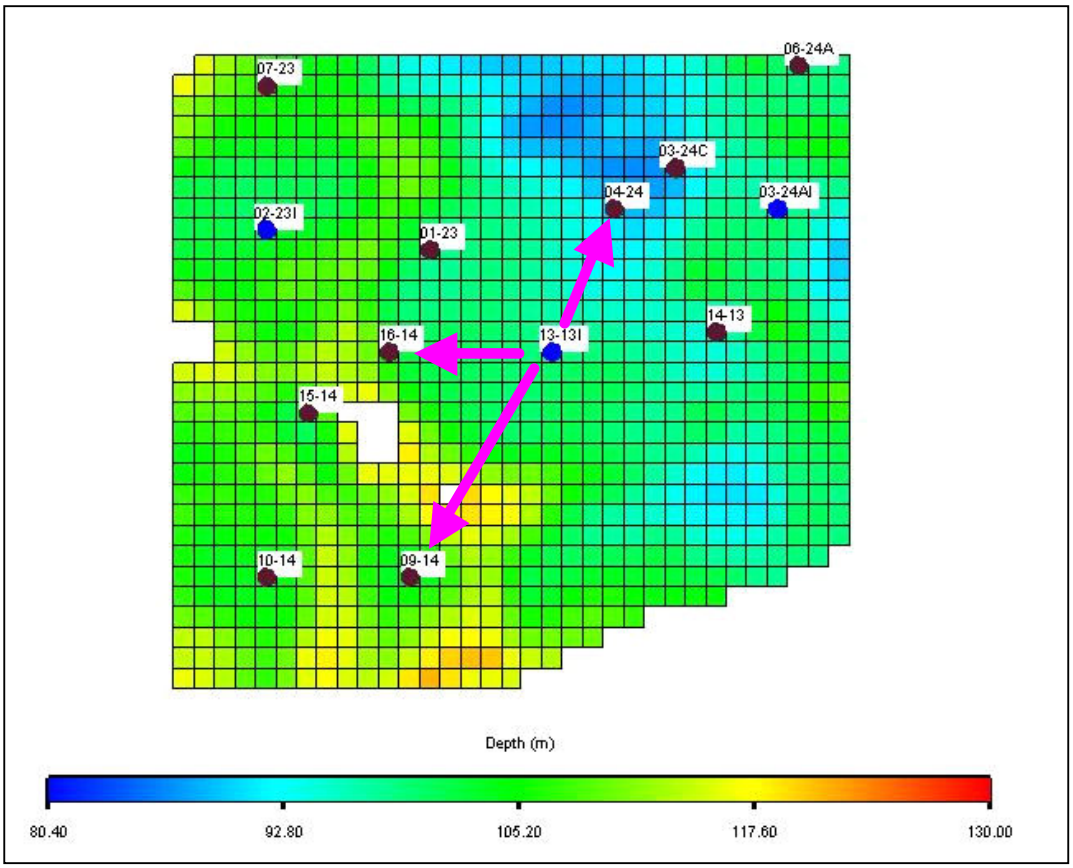

Figure 34 - Sinkhole Modelling. Dye Injection and Monitoring. Pattern 13-13-32-25W3M.

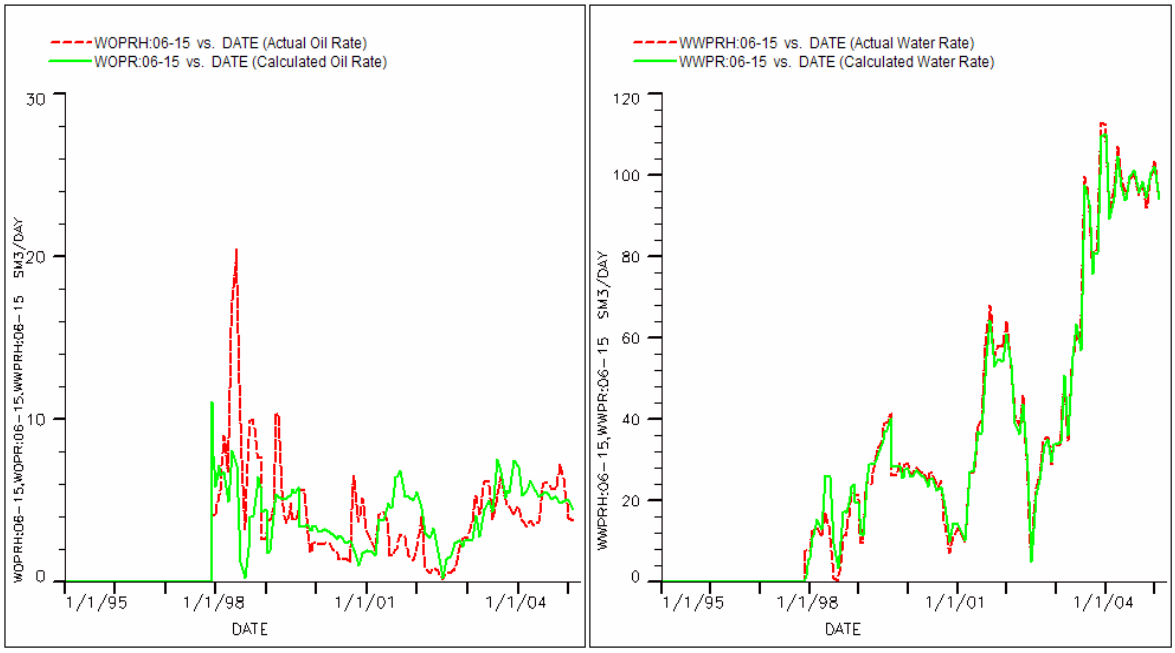

Figure 35 - History Match. Production Rates of 06-15-32-25W3M

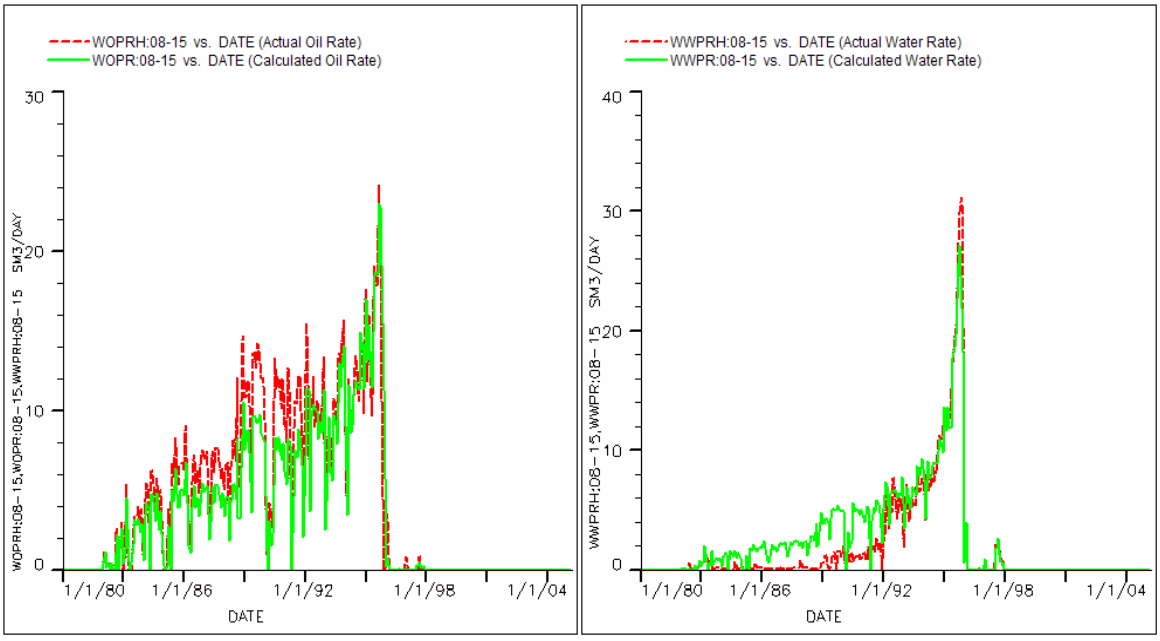

Figure 36 - History Match. Production Rates of 08-15-32-25W3M

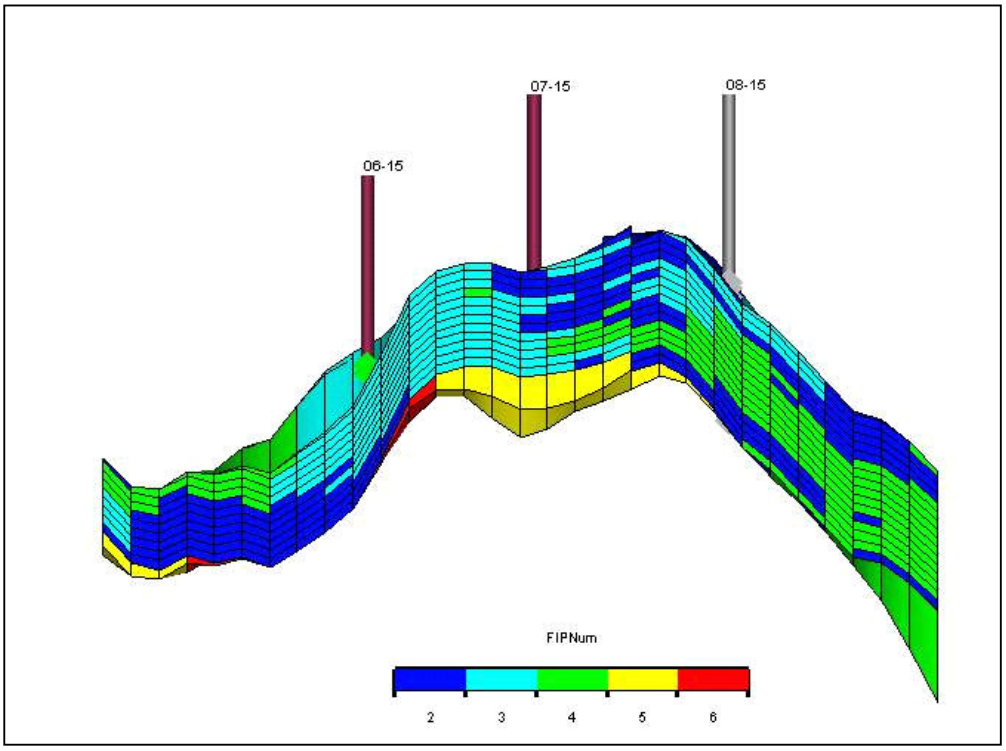

Figure 37 - E-W Cross Section. 08-15-32-25W3M. Facies Distribution

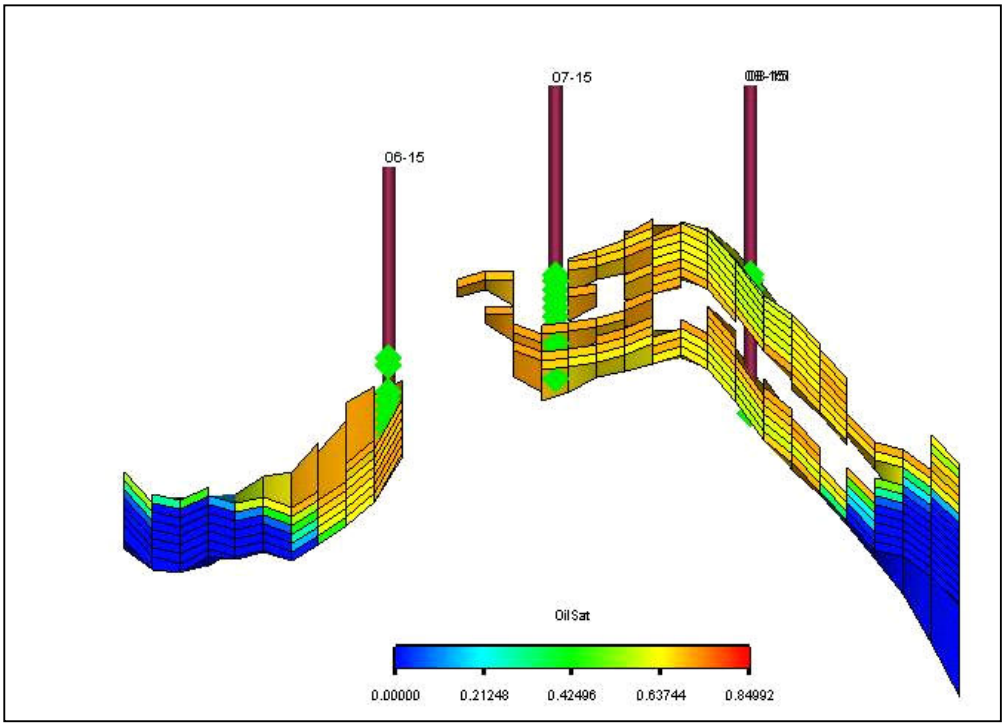

Figure 38 - E-W Cross Section. 08-15-32-25W3M. Blocks with Sw > Swf